2006

Models of Disordered Media and Predictions of Associated Hydraulic Conductivity

L. Aaron Blank Jr.
Wright State University

Models of Disordered Media and Predictions of Associated Hydraulic Conductivity

A thesis submitted in partial fulfillment
of the requirements for the degree of
Master of Science

By

L AARON BLANK
B.S., Wright State University, 2004

2006
Wright State University

WRIGHT STATE UNIVERSITY

SCHOOL OF GRADUATE STUDIES

Novermber 6, 2006

I HEREBY RECOMMEND THAT THE THESIS PREPARED UNDER MY SUPERVISION BY L Blank ENTITLED Models of Disordered Media and Predictions of Associated Hydraulic Conductivity BE ACCEPTED IN PARTIAL FULFILLMENT OF THE REQUIREMENTS FOR THE DEGREE OF Master of Science.

_____
Allen Hunt, Ph.D.
Thesis Advisor

_____
Lok Lew Yan Voon, Ph.D.
Department Chair

_____
Joseph F. Thomas, Jr., Ph.D.
Dean of the School of
Graduate Studies

Committee on
Final Examination

_____
Allen Hunt, Ph.D.

_____
Brent D. Foy, Ph.D.

_____
Gust Bambakidis, Ph.D.

_____
Thomas Skinner, Ph.D.

Abstract

In the late 20th century there was a spill of Technetium in eastern Washington State at the US Department of Energy Hanford site. Resulting contamination of water supplies would raise serious health issues for local residents. Therefore, the ability to predict how these contaminants move through the soil is of great interest. The main contribution to contaminant transport arises from being carried along by flowing water. An important control on the movement of the water through the medium is the hydraulic conductivity, *K*, which defines the ease of water flow for a given pressure difference (analogous to the electrical conductivity). The overall goal of research in this area is to develop a technique which accurately predicts the hydraulic conductivity as well as its distribution, both in the horizontal and the vertical directions, for media representative of the Hanford subsurface. The Hanford subsurface is a disordered sequence of ice-age flood deposits. It is known that concepts from percolation theory are well-suited to addressing transport problems in disordered media. The objective of this thesis was two-fold: (a) to implement techniques using critical path analysis from percolation theory for calculating the distribution of *K* values for soils with known characteristics, (b) to apply this technique to 53 sets of particle-size data and water retention characteristics taken from soils which represent the area in which the Technetium spill occurred. The research performed should be applicable to other contaminated sites under DOE supervision as well as being relevant for agriculture, climate models, mining and elsewhere.

TABLE OF CONTENTS

LIST OF FIGURES

LIST OF TABLES

Introduction

The purpose of the work described in this thesis is to develop a general approach for calculating fundamental flow properties of *disordered unsaturated* porous media from an experimentally obtained description of the medium. A disordered medium is one that is not uniform, at least at some spatial scale. An unsaturated medium does not have all its pore space filled with moisture. The terms space and volume will be used interchangeably in what follows.

The topic of the research undertaken here has broad applicability. For example, soils in which water flows easily and which also retain moisture are important in agriculture. Prediction of flow and retention of water in agricultural soils is critical for optimal yields. Another example is Heap leaching, a mining practice in which bacteria catalyze chemical reactions transforming ore to metal. Predicting water and air flow in mining heaps allows optimization of bacterial activity and maximization of ore yield. In the atmosphere, water vapor is the most important greenhouse gas and in most cases the chief carrier of thermal energy. Description of vapor phase transport of water across the soil-air interface, which is dependent on soil flow properties, is vital for the development of accurate global climate models (Opportunities in the Hydrologic Sciences1991). Finally, understanding flow in nuclear waste deposits in the subsurface is essential in evaluating risks arising from contaminant transport by water.

The fundamental difficulty for most researchers in this field is the treatment of disorder and heterogeneity. Here disorder is used to imply that particles are not orderly arranged (i.e. particles of a given size are not all found together, but instead are mixed up

at random with particles of other sizes). Disorder encompasses also particle and pore shapes as well as composition. Heterogeneity arises from a lack of uniformity in many soil features, such as typical particle sizes and porosity, and from the existence of mud cracks, animal burrows, and plant roots. Heterogeneity and disorder are introduced over a wide range of spatial scales from geological layering through depositional processes with effects on the distributions of particle and pore sizes on scales ranging from millimeters to kilometers.

Other difficulties arise in obtaining accurate data from experiments which are to be used as inputs in this model. Experiments are performed in both field situations (spatial scales of meters) and laboratory samples (spatial scales of centimeters). Thus there may be important differences between the media in the two types of experiments. Samples are easily deformed in the process of collection. It is notoriously difficult either to dry or wet a sample completely. Porosity is often determined by measuring the difference in water content at full saturation and under dry conditions. But measurements of this sort *on the same sample* performed by different Department of Energy National Laboratories (Los Alamos, Livermore, Argonne, etc.) have been shown (Or and Wraith, 2003, unpublished) to yield porosities that differed by as much as 20%, and that typically differed by 10%. If the goal of a research project is to predict the hydraulic conductivity of a medium as a function of its saturation, then it is important to know what the porosity of the medium is.

The subject of subsurface hydrology has a significant overlap with soil physics, and the flow of fluids through disordered porous media is often recognized in both fields, as well as in pure physics, as a fundamental physics problem that is not completely solved. A fundamental difficulty is simply the development of a reliable mathematical

model of the medium. No consensus exists regarding a unified means for calculating flow properties of porous media. An important advance in treatment of fluid flow in disordered porous media was the invention (Broadbent and Hammersley, 1957) and development (e.g., Stauffer, 1979) of percolation theory. A great deal of further development has occurred since Broadbent and Hammersley's original work (summarized in the reviews of, Berkowitz and Balberg, 1993; Sahimi and Yortsos, 1990, Hunt, 2001, 2005), and some of that progress is represented here. We first define the relevant terms used throughout this thesis.

Basic Terminology

Virtually all (solid) media are porous at some scale, but what is addressed here are media for which the pores range in size from microns to millimeters, e.g., soils and rocks. These pores combine in various ways to form interconnected pathways which permeate the medium and allow for the flow of moisture (or air). The ratio of the volume of the pores, V_p, to the total volume of the medium, V, is called the porosity φ. The ease of passage of liquid water through the medium is represented by a quantity called the hydraulic conductivity, or K. This depends in a complex way on the structure of the medium (pore space in particular) as well as the distribution of water in the pore space. Because it is comparatively easy to vary the concentration of water in a soil, K is typically written as a function of the soil saturation defined as the volume fraction of the pore space occupied by the water (or, more generally, any wetting fluid). If V_w is the volume of water in the medium, then the saturation $S = V_w/V_p$. Throughout the course of this document the term 'full saturation' will occasionally be used. This will refer to when S is equal to one. When dealing with saturation, it is common to define the moisture

content θ, as the volume fraction of water relative to the total volume of the medium: $\theta=V_w/V$. Thus, the saturation is related to the moisture content by the relationship

$$\phi S = \theta \qquad \text{(I1)}$$

The value of the saturation is dependent on both particulars of the soil, and the operant value of the air-water interfacial tension or pressure. This pressure, P, is normalized to the density of water, ρ, and the acceleration of gravity, g, and denoted by height $h = P/\rho g$. To understand the influence of h on the moisture content of a soil in a natural setting take the example of the unsaturated portion of a soil above a water table. The soil could be considered to be composed of many vertical capillary tubes, with the tubes' distribution of radii with volume matching that of the soil pores. If the bottom of the capillary bundle is now placed in the water table at atmospheric pressure (air pressure varies minimally with the depth in a soil), water will rise inside each tube to a specific height. This height is established when the attractive forces of the moisture with the walls of the tube cancel the weight of the water column. In particular, tubes having smaller radius will have a higher water column. Thus, the number of capillaries with water at a given height h above the water table will decrease with increasing h. In a laboratory experiment h can be manipulated by changing the air pressure, and waiting until the system comes to equilibrium.

Because the soil is not really a capillary bundle, the pressure-saturation relationship (also called the water retention curve) is hysteretic. A water-saturated soil subjected to some pressure h will not actually have its largest pores drain first, then the next-largest, and so on: this is because the water must be replaced by air. Without a continuous air-filled pathway to the pore in question, the pore cannot drain. A similar constraint operates during wetting of a dry soil, so the difference between wetting and

drying curves in the pressure-saturation relationship is related to the connectedness of the soil pores.

Derived Quantities

The basic parameters to be calculated are the hydraulic conductivity as a function of saturation, $K(S)$, and the saturation as a function of h, $S(h)$ (giving ultimately $K(h)$). The calculation of these quantities from basic soil physics data, such as the distribution of pore sizes and the porosity, has occupied many researchers for at least a century (e.g., Buckingham, 1907, Kozeny, 1927, Carman, 1956, Collis-George, Miller and Miller, 1956, Burdine, 1953, Millington and Quirk, 1959, Mualem, 1976, van Genuchten, 1980, Arya-Paris, 1981). As such, this is a problem of great interest in subsurface hydrology. These older works have been criticized on many grounds (e.g., Snyder, 1996, Hunt, 2004) and there are two chief areas of concern. One is that the usual means to generate the pore-size data from the particle-size data need not be unique, while the other relates to the difficulty in generating an effective transport property for a heterogeneous medium. The former problem is not addressed in this thesis, but the latter problem is. In particular the usual means of generating effective transport coefficients through taking arithmetic means of microscopic values are inaccurate in disordered systems. A better method (Seager and Pike, 1974) is to apply percolation theory in the form of critical path analysis (developed initially by Ambegoakar et al., 1971 and Pollak, 1972). This approach is used here and allows not only a better prediction of the hydraulic conductivity, but a less ambiguous evaluation of the suitability of any given model of a porous medium. This is the theoretical advantage of the work described here.

At the pore scale it is typical to assume that given a particle size/shape distribution and a porosity, one can generate a well-defined pore size/shape distribution (Arya and Paris, 1981, Gvirtzman and Roberts, 1991). This distribution is assumed to be stationary on a scale of centimeters, the typical size of a core sample of soil taken for measurements of K (i.e., the pore-scale disorder does not change over a relevant spatial scale). But such particle size distributions typically do change in space over a range of decimeters (or less) due, for example, to e.g., local heterogeneities in depositional environments or chemical heterogeneities in parent rocks from which soil weathers. Over larger scales (hundreds of meters) the chemical composition and even geologic origin of porous media can vary greatly, such as the variation between crystalline rock and recent flood deposits. Thus the hydraulic conductivity varies in space over orders of magnitude in a very complicated manner.

One of the first advances in modern soil physics was the recognition that the great complexity of real soils might be describable using the fractal models developed in the 1980's (Turcotte, 1986, Tyler and Wheatcraft, 1990, Rieu and Sposito, 1991, summarized in Baveye et al., 1998). These fractal models assume self-similarity (i.e., that the medium essentially looks the same on all length scales) and their application yielded various power-law relationships for pore and/or particle volume distributions as well as other properties, such as water retention curves. However, the simplification developed from these models did not appear adequate to address all of the discrepancies between theory and experiment. The purpose of applying percolation theory to fractal models (Hunt, 2005) has been to explain as many of the remaining deviations as possible between theory and experiment. Nevertheless it may be that not all soils follow a simple fractal law. In fact, in many cases (including a significant fraction of the soils considered here)

the particle size distribution is far too complicated to be considered fractal in nature, i.e. described by a simple power law. Thus a generalization of the medium is required, and that generalization is considered here. The chief practical advantage (compared with, e.g., Hunt (2005)) is that any pore-size distribution can be treated, rather than just an idealized mathematical model.

Specific Goals

The work described in this thesis can and will ultimately be applied elsewhere to the problem of Technetium (Tc) transport in the subsurface of the US Department of Energy Hanford site near Richland, WA. A large amount of "high risk" Technetium (^{99}Tc) in solution was intentionally discharged to ground at a specific location on the Hanford reservation called the BC Crib site (Ward et al., 2006). It is currently not known whether to expect this Tc plume to reach the Columbia river within years or within centuries, a question of significance to all who live downstream (Portland Oregon, for example). For this reason soils from that site with known K have been chosen, both for testing the validity of the code and the theory on which it is based and for making subsequent predictions in cases where K is unknown. The general strategy is to develop the best prediction of K at the core scale (using soil physics data, such as the porosity and the particle-size distribution), and use the statistics of the variability of the soil physics data and fundamentals of percolation theory to predict K at larger scales.

The specific purpose of this thesis is to solve the problem of finding $K(h)$ for an arbitrary medium by writing two pieces of code: 1) to calculate $\theta(h)$, the water retention curve as a function of interfacial tension (between wetting and non-wetting fluids), and 2) to calculate the hydraulic conductivity $K(\theta)$ of a particular soil as a function of

volumetric moisture content (θ). The ratio of K for a particular moisture content vs. K at full saturation (K_S) is calculated. If a measured value of K_S is available, then K as a function of θ can be plotted and compared with experiment (if that information is available).

The method of calculation chosen here is a generalization of the application of percolation theory to random fractal media mentioned above. To understand this application it is necessary to give some background information on percolation theory. In the theory section, calculations for a fractal medium are discussed as a special case of the more general method developed here.

Theory

Percolation theory has been successful in describing fluid flow in disordered media (Berkowitz and Balberg, 1993; Sahimi and Yortsos, 1990; Hunt, 2005). Imagine taking a pitcher of water and pouring it onto the surface of a rock. The rock is made up of solid volumes and empty volumes, called pores, which are of variable size and orientation with respect to each other. The size and location of one pore in the rock is often assumed to be independent from the size and location of other pores. A question that percolation theory attempts to address is the following: Does the water find a series of connected holes through which it can flow from the top of the rock to the bottom? That is, can the water *percolate* through the rock? (This example is closely related to the original work of Broadbent and Hammersley (1957), which grew out of research dealing with the performance of gas masks.) It should be mentioned that the strict definition of percolation is that connection is possible in all coordinate directions (Stauffer, 1979).

Percolation theory exists in three main forms: site, bond, and continuum. The type of percolation theory I will use to introduce the basic concepts is called site percolation theory, which is discussed next.

Site Percolation Theory

So, we now know the basic idea of percolation theory, but what is it exactly and how does it work? To begin answering this question, imagine a square lattice. That is, imagine a set of squares that are all the same size and compactly placed next to each other, similar to a piece of graph paper. Imagine that this lattice is so large that the

effects from the edges play a negligible role (thermodynamic limit, defined as allowing the number of squares in the lattice to go on infinitely so that there are no edges). Now, begin to put dots in the center of different squares. There are many ways to imagine placing these dots. For instance, they could *like* each other and want to be close to each other, or they could not like each other and want to have some space around them, but the simplest way to arrange the dots is by having them ignore each other. That is, the probability that one square contains a dot is *independent* from the probability that any other square contains a dot. This is the case in the original version of percolation theory. Also in its original version we have that the probability that a square contains a dot is the same for all squares in the lattice, and is denoted by p. As a consequence of the random or independent nature of the lattice, we have that the probability of a square being empty is $1-p$. When these dots are distributed throughout the lattice, certain lattice sites will not only contain dots themselves, but they will have nearest neighbors (that is, a square immediately left, right, above or below the square in question, but not diagonally proximate) which also contain dots. A group of s lattice sites which are all filled and all connected through neighboring sites is called a cluster of size s. If a cluster can be found which extends from one side of the lattice to the other, without any break in the chain, then the system is said to percolate. For our example above, if the dots represent pores in the rock and a cluster can be found that extends from the top of the rock to the bottom, then the water will be able to *percolate* through the rock. (The size of the pores which form the percolating cluster is going to affect 'how much' water will flow in a given amount of time, i.e. the 'conductance' of the percolating path.) From a strictly mathematical point of view, percolation theory deals with the statistics of these clusters (Stauffer, 1979, Wikipedia, "Percolation theory,").

A natural question that arises now is, "What is the relationship between the probability p that a lattice site is filled and the existence of a percolating cluster?" In fact, this is the main question percolation theory tries to answer, just re-cast in a different form. For low values of p it will be difficult to find a cluster which extends across the network. For high values of p one will almost certainly find a percolating cluster. So, where does the transition between these two cases occur? When dealing with any infinite lattice (thermodynamic limit) it turns out that there is a single value for p which defines the transition, denoted p_c for the critical probability or the percolation threshold. The probability of finding a percolating cluster is a step function, equaling zero if p is below the percolation threshold and one if p is above. This probability is discontinuous at $p=p_c$. The specific value of p_c depends not only on the dimensionality of the space, but also the geometry of the lattice. (Also, note that in the infinite lattice the percolating cluster will extend from any one 'side' of the lattice to any other 'side.' It is for this reason that there can only be one percolating cluster in an infinite lattice. For, if the cluster percolates in one direction, it will percolate in all directions.) For all values of p below p_c on such a network there will be no chance to find a percolating cluster, and for all values of p above p_c there will always be one percolating network (Fig T1). When dealing with lattices of finite size, however, p_c less sharply defines the existence of a percolating cluster (Fig T2). Sometimes for $p<p_c$ a finite cluster will extend across the system and for $p>p_c$ a finite-sized hole will extend across the system. However, as can be seen in Fig T2, p_c still represents a good measure of the critical value where the probability of finding a percolating cluster shifts from very low to very high. The major difference between the infinite lattice and the finite lattice is that the transition from no percolating cluster to a

percolating cluster occurs discontinuously in the infinite case and continuously in the finite case (Stauffer and Aharony, 1994).

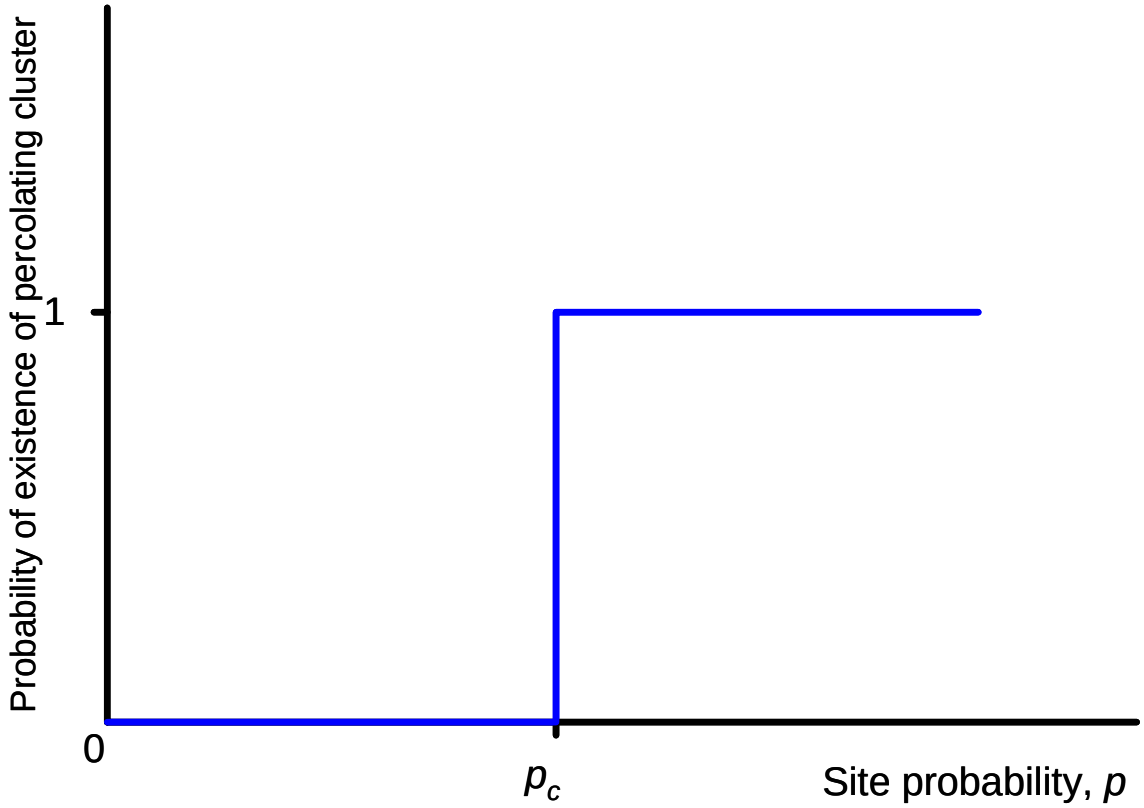

Fig. T1

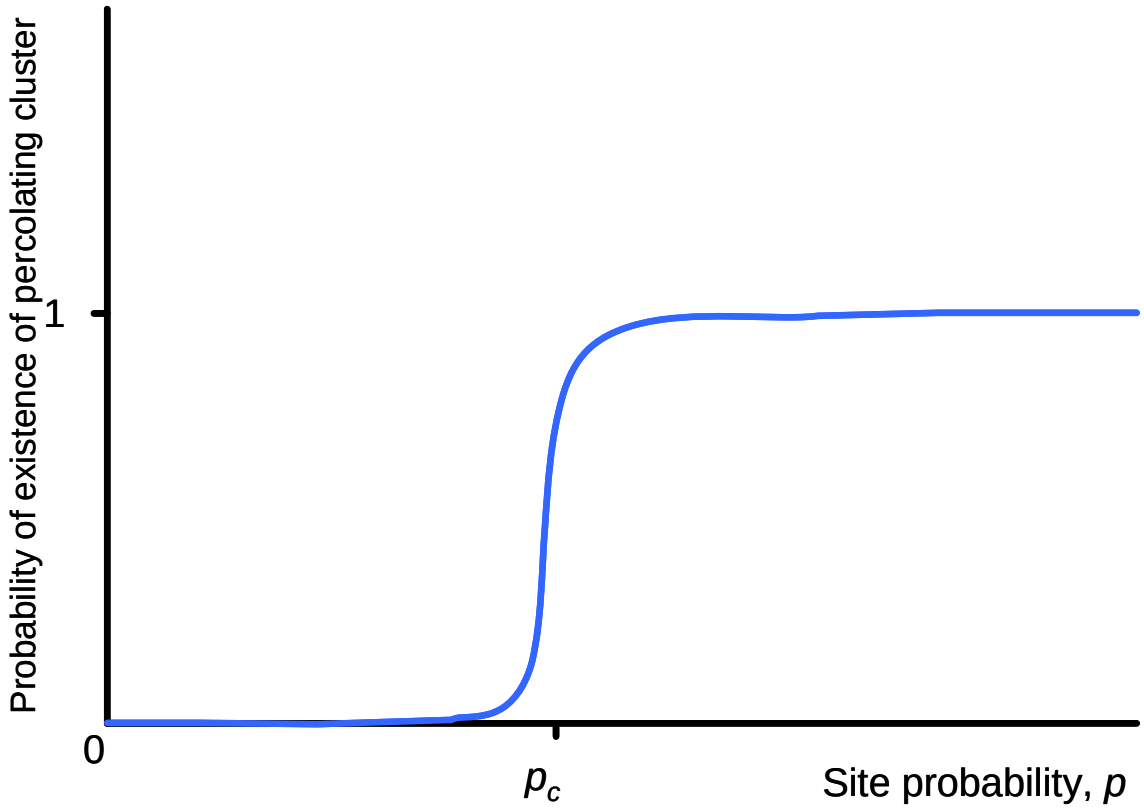

Fig T2

Now I would like to introduce some important quantities for the statistics of these clusters. Most of this discussion has its roots in the discussions in Stauffer (1979) and Stauffer and Aharony (1994). First let us define n_s equal to the number of clusters with s occupied sites divided by the number of sites in the lattice. Since there are s sites in the cluster, sn_s becomes proportional to the probability that if we point to a random site we hit a cluster of size s. If we sum sn_s over all values of s, then we get the probability p that a site is occupied. For ease of calculation the sum is approximated as an integral (Stauffer, 1979).

$$p = \int_{s=1}^{\infty} sn_s ds \qquad \text{(T1)}$$

Another important quantity in the cluster statistics is the idea of a correlation length, denoted χ. This quantity is important because it gives a measure of the scale of the lattice. The correlation length is effectively the distance across the largest finite cluster in the lattice. If p is less than p_c then there is no percolating cluster and the largest finite cluster will be the largest cluster in the lattice. As p approaches p_c from below the largest finite cluster is becoming the infinite cluster, so the correlation length tends to infinity. Now, if p is greater than p_c then there is an infinite cluster present, so the correlation length is defined as the distance across the largest cluster which is not infinite. As p gets closer and closer to one, more and more of the sites in the lattice are occupied and are therefore going to be connected to the infinite cluster, so the size of the largest finite cluster is going to decrease. Conversely, as p decreases from one and approaches p_c from above, fewer occupied sites are connected to the infinite cluster so the largest finite cluster is growing in size. Therefore, as p goes to p_c from above, the correlation length is again becoming infinite. This is a very important result in percolation theory, because it tells us that when we are at the percolation threshold, we lose any sense of scale we had in our lattice.

As stated above, the value of p_c is intimately connected to both the dimensionality of the space and the geometry of the lattice (i.e., whether it is hexagonal or square, for example). However, there are certain critical exponents in percolation theory which are geometry-independent. That is, they depend only on the dimensionality of the space. For example, n_s takes on the following form (Stauffer, 1979)

$$n_s = s^{-\tau} \qquad p = p_c \qquad \text{(T2)}$$

$$n_s = s^{-\tau} f(s^{\sigma}(p - p_c)) \qquad p \neq p_c \qquad \text{(T3)}$$

where both τ and σ are such critical exponents. If we consider the case where p equals p_c and plug in the value for n_s from eqn(T2) into integral (T1), we obtain

$$p_c = \int_{s=1}^{\infty} s^{1-\tau} ds \qquad \text{(T4)}$$

In order for this integral to converge, τ must be greater than 2. In fact τ=2.18 in three dimensions (Stauffer, 1979), independent of the geometry of the lattice, while σ=0.45 (Stauffer, 1979). There are several more critical exponents which all share this sole dependence on dimensionality (although these exponents are not independent of each other (e.g., Stauffer, 1979, Fisher, 1971)). This discussion is relevant to applying the present results to the transport of Technetium in Hanford site soils, but the details of this theory (Hunt, et al., 2006) are outside the scope of this thesis. Such basic theory is also relevant for finite-size effects when they are important. However finite-size (or edge) effects are important only in systems of ca. 50 particles on a side or larger (Hunt, 2001). For normal soils, with particle sizes in the micron to millimeter range, and core sizes approximately 5cm on a side, this does not present a problem. Thus, finite-sized systems are not considered in any portion of the following theoretical development.

There are many other types of lattices which we could apply site percolation to. For example, in two dimensions there can also be triangular and diamond lattices. Also, there's no need to restrict the analysis to two dimensions. In fact, the physical problems we want to tackle (including the problem addressed in this thesis) are in three dimensions. Further, it is also possible to have more than one kind (or "species") of occupied site, analogous to different colored dots in the centers of the squares. In order for a particular species to percolate a path must be connected through sites of that "color"

alone. Since percolation requires simultaneous connections between all borders of a medium, in two dimensions it is only possible for one species of occupied site to percolate as the one percolating cluster of any species cuts off all other clusters. In three dimensions connections can avoid a block in any particular plane and multiple clusters can percolate. In a porous medium the different colors could correspond to different immiscible fluids (water, air, oil). There are also two more entirely different kinds of percolation theory, one which deals not with sites in a lattice but with bonds between sites, and another called continuum percolation (Scher and Zallen, 1970). I will describe continuum percolation next in greater detail in the context of its application to relevant soils.

Continuum Percolation Theory

The particular form of percolation theory called continuum percolation is of greatest relevance to problems involving porous media. An argument for this is that soil particles often vary in size by over two orders of magnitude or more, rendering lattice descriptions inappropriate. In continuum percolation theory the relevant variable is a volume, rather than a site or bond fraction, and the relevant questions relate to the connectivity of some particular type of volume, such as solid particles, pore volumes, or volumetric fluid contents. All of these species can percolate simultaneously,

As a specific application then, Continuum Percolation Theory tells us that if a certain critical fraction of the pore space is saturated, then there will exist a percolating path of water-filled pore space extending from one side of the system to the other. Such a connected path is essential not only for fluid flow, but for molecular diffusion of a solute as well. In the absence of such a connected path through water-filled pore space, the

physical process of diffusion cannot bring a solute from one side of a medium to the other. Thus it is known that such quantities as the diffusion constant or the conductivity (electrical, thermal, or hydraulic) must vanish at the percolation threshold and be identically zero below the threshold. The fact that this predicted behavior is observed for solute diffusion in porous media (which indeed vanishes at a specific moisture content, Moldrup et al., 2001) is a strong motivation for taking an approach based on percolation theory, especially since experiment shows that even in sedimentary rocks, over ninety-nine percent of the pore space is interconnected (Sahimi, 1993). However, the most important application of percolation theory in water flow in porous media, at least over most of the range of experimentally accessible saturations, is critical path analysis (Ambegaokar et al., 1971; Pollak, 1972). Critical path analysis calculates the path of least resistance through the medium. It is usually applied far above the percolation threshold in order to isolate that part of the medium which contributes most to the macroscopic flow (or current). It is known to be the most accurate means for calculating effective transport coefficients in highly disordered media (e.g., Seager and Pike, 1974). This method was not discussed in the standard review (Berkowitz and Balberg, 1993), which may help to explain why it has not yet been applied generally.

To get a better feel for what critical path analysis does, consider a soil with moisture well above the percolation threshold. In such a medium, there will be many different percolating paths which a volume of moisture might take in its journey from one side of the system to the other. Each of these paths can be considered in parallel, using an analogy to an elementary electric circuit of resistors set up in parallel. One argues that the percolating path with the least resistance (or highest conductivity) will dominate the overall resistance of the circuit.

The pores along the path of least resistance can be thought of as resistors connected in series. Since the resistance of a pore increases as its cross-sectional area decreases, the resistance of the chain of pores will be dominated by the resistance of the smallest pore (largest resistor) in the chain. The effective radius (for flow) of this smallest pore along the critical path is called r_c. Thus the largest resistance (smallest pore) on the most conducting path dominates the expression for K for the medium.

When a soil is in equilibrium, the moisture will all collect in the smallest pores possible (standard texts on soil physics, e.g., Marshall et al., 1996). The largest pore that can be filled with water is denoted $r_>$ and, under equilibrium conditions, all pores smaller than $r_>$ are filled with water. Over the small size of lab samples effects of gravity are typically ignored. Gravity induced variations in h are on the order of the sample height, typically 5-10cm whereas the experimental variations treated here extend over thousands of centimeters. $r_>$ will, in general, be a function of saturation, S. Similarly, all pores larger than $r_>$ contain air. In a real soil, this condition may be violated for several reasons: 1) the path which a fluid may need to follow to exit (or enter) the medium contains pores which the fluid would not reside in under equilibrium conditions (because e.g., $r>r_>$, the largest pore which can be filled with water, 2) the rate at which the fluid enters or exits the medium is so slow that the change in moisture content would take centuries or longer.

Applications

Next, I consider the application of Continuum Percolation Theory to a simple fractal model of a soil, which provides the background for the more general results presented in this thesis. Fractal models for soils were introduced by Turcotte (1986) and

others (e.g., Tyler and Wheatcraft, 1990), but the particular model used here is adapted from Rieu and Sposito (1991) by Hunt and Gee (2002a). In this model the pore space is represented by one fractal with dimensionality D_p and the particle space is modeled with a different fractal with dimensionality D_s. The ideas motivating the development of this analytical example can be extrapolated to apply to any particle/pore size distribution (psd), but use of this specific example is illustrative, and also gives a comparative theoretical result in case the particular material investigated is compatible with this simple model.

The expression, $W(r)dr$, is proportional to the probability density function (pdf) that an arbitrary pore has radius between r and $r+dr$. For ease of communication, $W(r)dr$ in this context will be referred to as a pdf, even though it describes a relative rather than an absolute probability. In particular, for a fractal model, we have (Hunt and Gee, 2002a),

$$W(r) = \frac{3 - D_p}{r_m^{3-D_p}} r^{-1-D_p} \qquad r_0 \le r \le r_m \qquad \text{(T5)}$$

where r is the dimension of the pore, r_m is the maximum pore size in the medium, r_0 is the minimum pore size, and D_p is the fractal dimensionality of the pore space. Under the assumption that volume is proportional to r^3, $r^3W(r)dr$ represents the fraction of the total volume occupied by all the pores between size r and size $r+dr$. The particle space is represented by a similar pdf obtained by exchanging D_p by D_s. D_p and D_s are not independent quantities (Hunt and Gee, 2002b).

The integral of $r^3W(r)$ between two general limits r_1 and r_2 appears repeatedly in what follows, defining many useful quantities for any soil model defined by a pdf $W(r)dr$. For the particular case of a fractal model given by Eq. (T5),

$$\int_{r_1}^{r_2} r^3 W(r) dr = \left(\frac{r_2}{r_m}\right)^{3-D_p} - \left(\frac{r_1}{r_m}\right)^{3-D_p} \qquad \text{(T6)}$$

Applying Eq. (T6) to the case $r_1 = r_0$ and $r_2 = r_m$ gives the fraction of the total volume occupied by all of the pores in the medium. This is the definition of the porosity, φ, given earlier so that in the fractal case,

$$\phi = 1 - \left(\frac{r_0}{r_m}\right)^{3-D_p} \qquad \text{(T7)}$$

This result for φ is the same as that obtained by Rieu and Sposito (1993), even though they used a model with only discrete pore sizes allowed. Notice that the geometry of the pores is not taken into consideration when expressing the volume of the pore as r^3. This has no impact on the results for two reasons. First, the geometrical constant is the same for all pores due to the self-similarity of the fractal. And second the pore radii enter in as a ratio and any such constant will cancel. Note that when we calculate the ratio of the hydraulic conductivity at a certain water content vs. the hydraulic conductivity at full saturation a similar ratio of geometrical constants will also cancel (as described below).

Since any infinitesimal volume in the soil must either belong to the pore space or the particle space, $1-\varphi$ must be the fractional volume occupied by the particle space. Looking at the above equation we see that if we change D_p to D_s then we are integrating the pdf for the particle space. Therefore, our results remain valid under a substitution of D_s for D_p in any of our equations as long as it will be accompanied by a substitution of 1-φ for φ. This gives,

$$\phi = \left(\frac{r_0}{r_m}\right)^{3-D_s} \qquad \text{(T8)}$$

This result is identical to that of Nigmatullin et al. (1992). This shows that the porosity can be expressed in terms of the fractal dimensionality of the particle space. It therefore enters below into the equation for the surface area to volume ratio of the particle space.

The value of the critical moisture content required for percolation, θ_t (t is for threshold as in 'percolation threshold') has been determined experimentally to be (Moldrup et al. 2001),

$$\theta_t = 0.1905\left(\frac{A_s}{V}\right)^{0.52} \qquad \text{(T9)}$$

where A_s/V is the ratio of the surface area of the particle space to the volume of the particle space. In eqn(T9) A_s/V was determined experimentally by gas adsorption. A value of A_s/V can also be estimated from (Hunt and Gee, 2002a)

$$\frac{A_s}{V} \propto \frac{\int_{r_0}^{r_m} r^2 W(r)\,dr}{\int_{r_0}^{r_m} r^3 W(r)\,dr} \qquad \text{(T10)}$$

In Hunt and Gee (2002a) it was assumed that the calculated value of A_s/V in eqn(T10) was proportional, at least, to the measured A_s/V in eqn(T9) and a regression coefficient was found by comparison to experiments. Here the fractal dimensionality for the solid particles is used because the calculation addresses the solid surface and the solid volume. Because the geometry of the pores is not known, eqn(T10) uses r^2 for a particle surface area as well as r^3 for its volume, with no specific shape assumed.

Turning to the hydraulic conductivity, first define the moisture content, θ, of a soil, irrespective of whether the water percolates or not. The minimum water content

necessary for percolation (the threshold value) is denoted as θ_t. Applying our general result Eq. (T6) to the case $r_1 = r_0$ and r_2 equal to the largest pore with moisture, $r_>$, gives

$$\theta = \left(\frac{r_>(S)}{r_m} \right)^{3-D_p} - \left(\frac{r_0}{r_m} \right)^{3-D_p} \qquad \text{(T11)}$$

which yields the volume fraction of the moisture, by definition the moisture content. In this result and the following results we have explicitly represented the fact that $r_>$ is a function of saturation. Making the substitution of $S\varphi=\theta$ from eqn(I1) results in

$$S = \frac{1}{\phi} \left[\left(\frac{r_>(S)}{r_m} \right)^{3-D_p} - \left(\frac{r_0}{r_m} \right)^{3-D_p} \right] \qquad \text{(T12)}$$

Remember that the largest resistance (smallest pore) on the most conducting path dominates the expression for K for the medium. So consider a soil which is at the critical moisture content, θ_t, for percolation. The saturation, which ranges from zero at completely dry to 1 at completely wet, will be some critical or threshold value, S_t. Such a soil contains moisture in all pores from size r_0 to the largest pore size which still has water, denoted $r_>$, and θ_t is equal to the moisture content, eqn(T11), for the specific case of a percolating soil at saturation S_t. As the saturation (equivalently moisture content) increases, so that $S>S_t$, $r_>$ will increase. In order to force the integral in eqn(T6) to yield θ_t for the new saturation, the lower limit must become greater than r_0 and it will depend on S. This lower limit then defines r_c (the largest resistance on the most conducting path) as a function of saturation. Although it is possible to choose a smaller value for the lower limit (with the upper limit smaller than $r_>$) this percolating path would have a much larger resistance due to the smaller pores included on the path. Performing the integration in Eq. (T6) gives

$$\theta_t = \left(\frac{r_>(S)}{r_m}\right)^{3-D_p} - \left(\frac{r_c(S)}{r_m}\right)^{3-D_p} \qquad \text{(T13)}$$

If one integrates instead eqn(T11) from r_0 to $r_>$ then one still gets the total moisture content of the percolating soil, but this is now greater than θ_t. As S goes to 1, $r_>$ goes to r_m and $r_c(S)$ goes to $r_c(S=1)$. As stated before, it is the smaller pores which provide the bottlenecks in the percolating cluster since they have larger resistances (Hunt and Gee, 2002b). The significance of r_c increasing with saturation is that the pore size which bottlenecks the conductivity increases with saturation, ie., the conductivity increases. Even though the pores smaller than r_c contain liquid and have larger resistances to flow, they are not necessary to form a percolating cluster and therefore do not hinder the conductivity. In the case where the soil is saturated ($r_> = r_m$), we see that

$$\theta_t = 1 - \left(\frac{r_c(S=1)}{r_m}\right)^{3-D_p} \qquad \text{(T14)}$$

These simple results yield most of the information necessary to calculate the ratio of $K(S)$ to $K(S=1)$. What is still needed is a way to find an appropriate conductance of a pore from its radius, since critical path analysis identifies the critical conductance (or equivalently, resistance). In order to write down the conductance of a pore it is necessary to find the flow through a pore for a given pressure difference (analogous to the electrical current for a given potential difference). This result for an arbitrary pore shape is difficult to obtain. But for the present (fractal) case, all that is needed is how the flow scales with pore radius r. Such a result for the flow for a right circular cylinder is given by Poiseuille's law for viscous flow (Halliday et al., 2004), which states that the flow is proportional to r^4/L, where L is the length of the cylinder. For fractal media L must, in the

mean, be proportional to r, making r^4/L proportional to r^3. There is no guarantee that this particular power must be appropriate if a medium is not fractal (e.g., if the pore-size distribution is not a simple power law). Nevertheless this simplest assumption possible is chosen since there is no evidence on which to base a more complicated model (which would require a distribution for L). This assumption yields verified results (Hunt and Gee, 2002b) when the soil is a fractal. Armed with the assumption that the hydraulic conductivity is proportional to the cube of the critical pore size we take the ratio of $r_c(S)$ to $r_c(S=1)$. After cubing we notice this is the ratio of the critical volume size at an arbitrary saturation vs. the critical volume size at full saturation. It is here that the geometrical constants in the volume cancel. Using T13 and T14 in the following steps we calculate,

$$\frac{r_c(S)}{r_c(S=1)} = \left[\frac{\left(\frac{r_>}{r_m} \right)^{3-D_p} - \theta_t}{1-\theta_t} \right]^{\frac{1}{3-D_p}} \qquad \text{(T15)}$$

Rearranging eqn(T12) for the saturation we have

$$\left(\frac{r_>}{r_m} \right)^{3-D_p} = \phi S + \left(\frac{r_0}{r_m} \right)^{3-D_p} \qquad \text{(T16)}$$

Using Eq. (T7)) for $(r_0 / r_m)^{3-D_p}$ gives

$$\left(\frac{r_>}{r_m} \right)^{3-D_p} = \phi S - \phi + 1 \qquad \text{(T17)}$$

Inserting eqn(T17) into eqn(T15) for the ratios of the critical pore size we find

$$\frac{r_c(S)}{r_c(S=1)} = \left[1 + \frac{\phi(S-1)}{1-\theta_t}\right]^{\frac{1}{3-D_p}} \qquad \text{(T18)}$$

Cubing r_c to obtain the hydraulic conductivity, as described previously, gives

$$\frac{K(S)}{K(S=1)} = \left[1 + \frac{\phi(S-1)}{1-\theta_t}\right]^{\frac{3}{3-D_p}} = \left[\frac{1-\phi+\theta-\theta_t}{1-\theta_t}\right]^{\frac{3}{3-D_p}} \qquad \text{(T19)}$$

At this point, it must be emphasized that eqn(T19) is obtained only for $W(r)$ appropriate for a fractal soil.

It is important to note that the derivation of eqn(T19) yields a valid expression for *K(S)* only for water contents high enough that the connectivity of the water-filled pores is not changing rapidly with saturation, i.e., so long as the percolation threshold is not approached too closely (from above). The basic problem in that case is that the correlation length from continuum percolation theory starts to diverge, meaning that the interconnected paths along which water can flow are becoming infinitely far apart. This represents a dominance of the role of connectivity vis-à-vis pore size distributions. Even if these flow paths are optimal, the total flow through the medium must be vanishing if their separation diverges. In such cases a universal expression (independent of the pdf) for *K(S)* from percolation theory applies (Berkowitz and Balberg, 1993, Hunt, 2005) which describes the effects of the rapid change in connectivity of the water-carrying paths.

The value for the moisture content which defines the transition between applying critical path analysis and the universal result for percolation theory has been calculated for the fractal model, but not in the general case. One of the principle new results in this thesis is the development of an algorithm to determine the relative impacts of

connectivity and of the pore size distribution on K for an arbitrary pore-size distribution. But in order to be explicit, first consider the effect for the fractal model.

When the pore size distribution is not relevant for K (θ is close to θ_t) it is known (Berkowitz and Balberg, 1993) that K must obey universal behavior, e.g.,

$$K(\theta) = K_0(\theta - \theta_t)^2 \qquad \text{(T20)}$$

where K_0 is, in principle, an unknown constant with units of hydraulic conductivity. Since eqn(T19) must hold for large saturation, but eqn(T20) must hold near the critical saturation, there must be a cross-over moisture content, called θ_d, which delimits the ranges of validity of these two equations. $K(\theta)$ and $dK/d\theta$ from eqn(T19) and eqn(T20) are set equal at $\theta = \theta_d$, yielding both K_0 and θ_d. Such a cross-over has the physical relevance of determining the ranges of moisture contents for which the pore-size distribution and the universal features of percolation theory are dominant respectively. For the fractal case the result of the above procedure for the cross-over moisture content is (Hunt, 2005)

$$\theta_d = \theta_t + \frac{2(1-\phi)}{\frac{3}{3-D_p} - 2} \qquad \text{(T21)}$$

This procedure is easily generalized to the non-idealized soils that are considered in this thesis. Instead of using eqn(T19) for the functional form for the hydraulic conductivity (a result specific to fractal geometry), K is set to the unspecified (and thus general) form $K(\theta)$. Then, combining this K with eqn(T20) and then setting $K(\theta)$ and $dK/d\theta$ equal for each equation when $\theta = \theta_d$ yields,

$$\theta_d = \theta_t + \frac{2K(\theta_d)}{\left.\frac{dK}{d\theta}\right|_{\theta=\theta_d}} \qquad \text{(T22)}$$

This is the *fundamental new* analytical formula of this thesis which will be employed below in the Data section.

At moisture contents below θ_d, most systems are not in equilibrium (Hunt and Skinner, 2005). Thus the discussion of water-retention curves below is typically restricted to moisture contents $\theta > \theta_d$. This also will imply that there can be no expectation that theoretical predictions will be verified for moisture contents $\theta < \theta_d$. We now turn our attention to the water retention curve ($\theta(h)$ from the introduction) of the medium.

Vital to our derivation of the water retention curve is the Young-Laplace relationship (e.g., Marshall, et al., 1996), which says the pressure, h, is inversely proportional to the largest pore containing moisture, $r_>$. The constant of proportionality we call A, so that $h = A / r_>$. h_A is defined to be that value of h such that air can just enter the largest pore in the medium, and this physical condition corresponds to $r_> = r_m$, Under these conditions (or any smaller value of h) the medium is fully saturated, $S = 1$. Applying Eq. (T6) to the saturation, Eq. (I1), for this case gives

$$S = \frac{1}{\phi}\left[\left(\frac{A/h}{r_m}\right)^{3-D_p} - \left(\frac{r_0}{r_m}\right)^{3-D_p}\right] \qquad \text{(T23)}$$

In eqn(T23) make the substitution $A/r_m = h_A$. Then add and subtract 1 inside the square brackets in eqn(T23) to generate φ-1 (from eqn(T7)). Then remove the term φ from the square brackets to yield

$$S = 1 - \frac{1}{\phi}\left[1 - \left(\frac{h_A}{h}\right)^{3-D_p}\right] \qquad \text{(T24)}$$

The procedure to find the water retention curve in the general case is to substitute the appropriate form of $W(r)$ into the above equations.

Details of the new procedure developed in this thesis for an arbitrary pore size distribution are given in the next section.

Data

In order to predict the hydraulic conductivity and the water retention curve of a given medium it is necessary to know the corresponding pore-size distribution, as illustrated above for the specific case of a fractal distribution. The quality and availability of experimental data on pore-size distributions is limited, as are the data for unsaturated hydraulic conductivity necessary for a comparison between theory and experiment. Most particle size data sets in the literature provide data points for only three different sizes (see, e.g., Marshall et al., 1996), which is insufficient to justify use of an accurate numerical routine. Among the data sets that do contain sufficient information, we describe next the assumptions that allow us to derive a pore-size distribution for predicting the hydraulic conductivity and water retention curve. The validity of these assumptions is assessed by comparing our theoretical predictions with experimental measurements of hydraulic conductivity and water retention below.

$W(r)$ for the pore size distribution (psd) is almost always unknown for a real soil. However, the integrated value $r^3W(r)$ (see eqn(T6)) for the *particle* size distribution (ie., the cumulative mass distribution, cmd) may be obtained from data specific to a given soil site under investigation. A simplifying assumption can then be made that the particle size distribution is proportional to the pore size distribution. The pore size, r, is assumed to be related to the particle size, R, by the following relationship (e.g., Arya and Paris, 1981, Gvirtzman and Roberts, 1991),

$$r = C * R \qquad \text{(D1)}$$

In our application we set $C = .3$ in accordance with the literature. Thus, the cumulative mass fraction at a given particle size gives the cumulative pore space at the corresponding pore size. This cumulative psd is equivalent to the integral on the left hand side of eqn(T6) with limits $r_1 = r_0$ and $r_2 = r$, i.e.,

$$\int_{r_0}^{r} r'^3 W(r')dr' = \text{cumulative psd}(r) \qquad \text{(D2)}$$

Furthermore, the discussion following eqn(T6) in the Theory section can then be used to obtain the moisture content and saturation. $S(h)$ can also be inverted numerically to find $h(S)$, which is a common representation of experimental data. Note that use of experimental data to generate the cumulative pore size distribution, as shown in eqn(D2), is the fundamental advance of this thesis relative to prior work applying critical path analysis (Hunt, 2005).

The cmd's were obtained from the US DOE Hanford site and supplied by Dr. Rockhold from Pacific Northwest National Laboratory (Rockhold et al., 1988; personal communication, 2005). Particle size distributions are typically obtained by a combination of sieving (for particles larger than 70μm) and by Stokes' settling for smaller particles. The data we received sometimes implied that the cmd is a non-monotonically increasing function of particle size, which would imply negative mass (realistically, lost mass) for particles in a given size range. For this reason such curves were dropped from further analysis.

The next issue that must be addressed is that the experimental data provide the cmd at discrete measured values of the particle radius. Interpolation between data points requires an assumption regarding the functional dependence of the cmd on the particle size. Due to the process of sieving discussed above, a step function was chosen, i.e., we

consider any particle size between two data points as equally likely to contribute to the cumulative mass fraction. This need not be the case; the functional dependence could be assumed linear or quadratic and the predictions could be analyzed to see if they yield better results. Even with a step function, a choice must be made on how to bin the data. For the i^{th} value R_i, the corresponding cmd could include all particles of size less than R_i. If this is assumed, then cmd_i becomes the value of the step function between R_{i-1} to R_i, where R_{i-1} is zero when $i = 1$ (i.e. the smallest particle size in the distribution goes to zero). Or it could include all particle sizes up to the next highest particle size (the step function equals cmd_i between R_i to R_{i+1} and R_1 is the smallest particle size in the distribution). These two ways of assuming the step function were implemented in the calculation of the hydraulic conductivity as extreme cases, which provide bounds for the results obtained from any intermediate interpretation (eg, linear interpolation between data bins). Since there was little difference in the result for K using these two extremes, we only implemented the second of these two interpretations in the calculation of the water retention curves.

Verification of the theoretical predictions for the water retention curve and hydraulic conductivity requires comparison with experimental data. Experimental water retention curves for the same soils used to obtain the cmd/psd were obtained in the laboratory using ceramic plates (Gee and Bauder, 1986) in a pressure chamber. The results yield the water content as a function of h. The data for the porosity (Ward et al., 2006) were obtained by measuring bulk density and assuming a value of the density of the individual particles.

The data for the hydraulic conductivity were obtained from field experiments and, together with the corresponding cmd's, were published in Rockhold (1988).

Code

Water Retention

In the data for the water retention curves cited above, pressure is the independent variable, as in eqn(T24) giving $S(h)$ for the fractal distribution. When filling up with liquid, the smallest pores in the soil are filled first, and when drying, the largest pores are evacuated first. The pore radius $r_>$ which delineates the boundary between water-filled and empty pores is inversely proportional to the value of the pressure (refer to discussion preceding eqn(T24)).

$$r_> = A / h \qquad \text{(C1)}$$

The proportionality constant A is a parameter which depends on the geometry of the pores. Since this geometry is unknown, A becomes an adjustable parameter used to fit the predicted curve to the data. A is the only adjustable parameter that will be used. For each value of pressure given in the data we calculate the corresponding $r_>$ using eqn(C1). As described in the Data section, when the integration limits in eqn(T6) are $r_1 = r_0$ and $r_2 = \underline{r_>}$, the cumulative pore size distribution inferred from the supplied particle cmd gives a theoretical prediction for the moisture content.

The data also provide experimental measurements of the moisture content as a function of pressure. The inverse, $h(\theta)$, is plotted along side the water retention calculation, so one can compare the prediction to the experiment. The following flow charts give the algorithm for calculating $h(\theta)$,

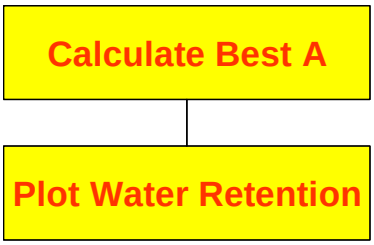

Breaking down Calculate Best A we have the following set up. Calculate Best A reads in the pore-size distribution and predicts a trial $h(\theta)$, which is then compared with experiment (via method of least squares). This function needs inputs of a minimum A, a maximum A and a value of how much to increment A. Calculate Best A then returns both the best value of A (defined as having the minimum least squares deviation) and the corresponding water retention prediction. The Plot Water Retention routine accepts both the calculated and measured curves and plots them. The next discussion gives the details.

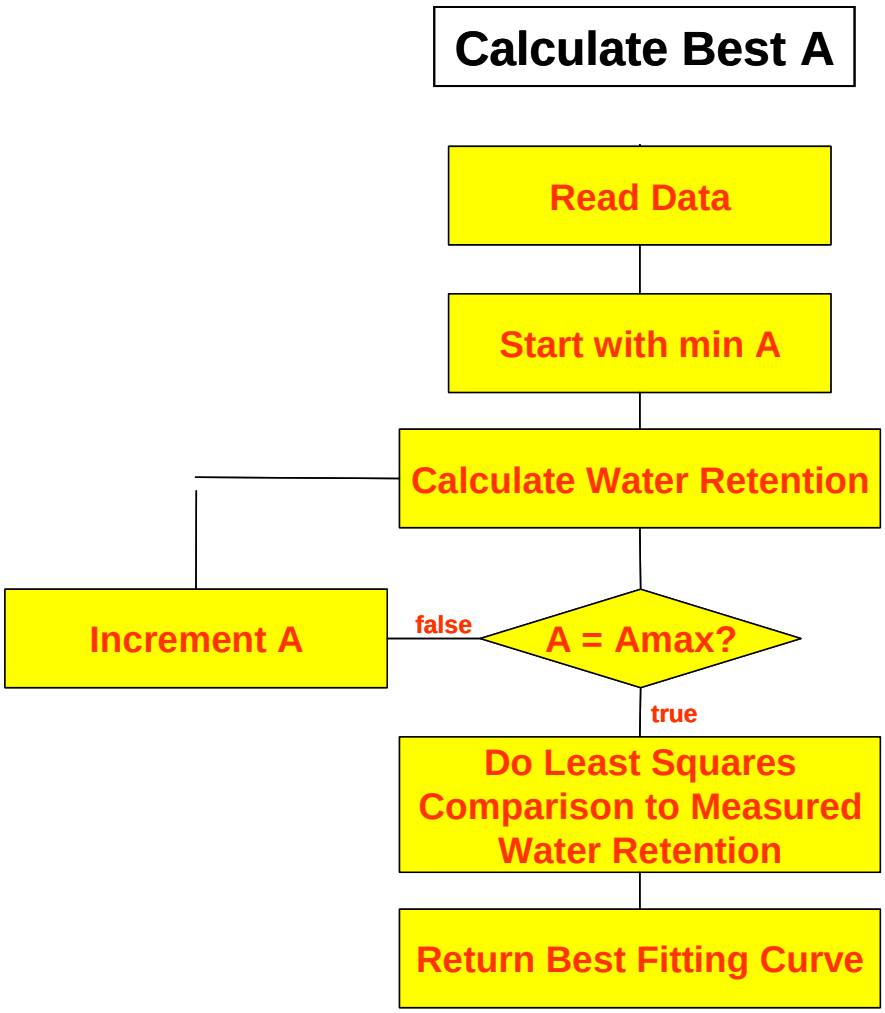

Read data reads particle-size data and the experimental water retention curve from a text file. It reads in the cumulative mass fraction as a function of particle sizes and the pressure as a function of water retention. Then we start with $A_{\min}$ and call Calculate Water Retention. This function takes in the data read from the file, along with a particular A value for which we calculate the water retention curve. It returns the predicted water retention curve (see further details, below). We then increment A and calculate the next curve, repeating this process until we reach $A_{\max}$. Once we are finished we compare every curve we calculated to the measured water retention curve and find the one with the minimum least squares deviation. While it cannot be excluded that the

extreme value of the least squares deviation could occur for the endpoints, A_{min} or A_{max}, in our particular case examination of the results shows that the values returned were always contained between these limits. We return this curve along with the experimentally measured curve. When doing this comparison we only compare up to a specified value of pressure (in this case log[h]=2.5), which corresponds to a minimum moisture content. In other words, the least squares routine calculates the squares of the deviations only for lower pressures. The reasoning behind this is that as the moisture content approaches θ_d (see eqn(T22)), the system being measured goes out of equilibrium, and we don't expect our prediction to agree with experimental results in this range.

Finally we break down the Calculate Water Retention routine,

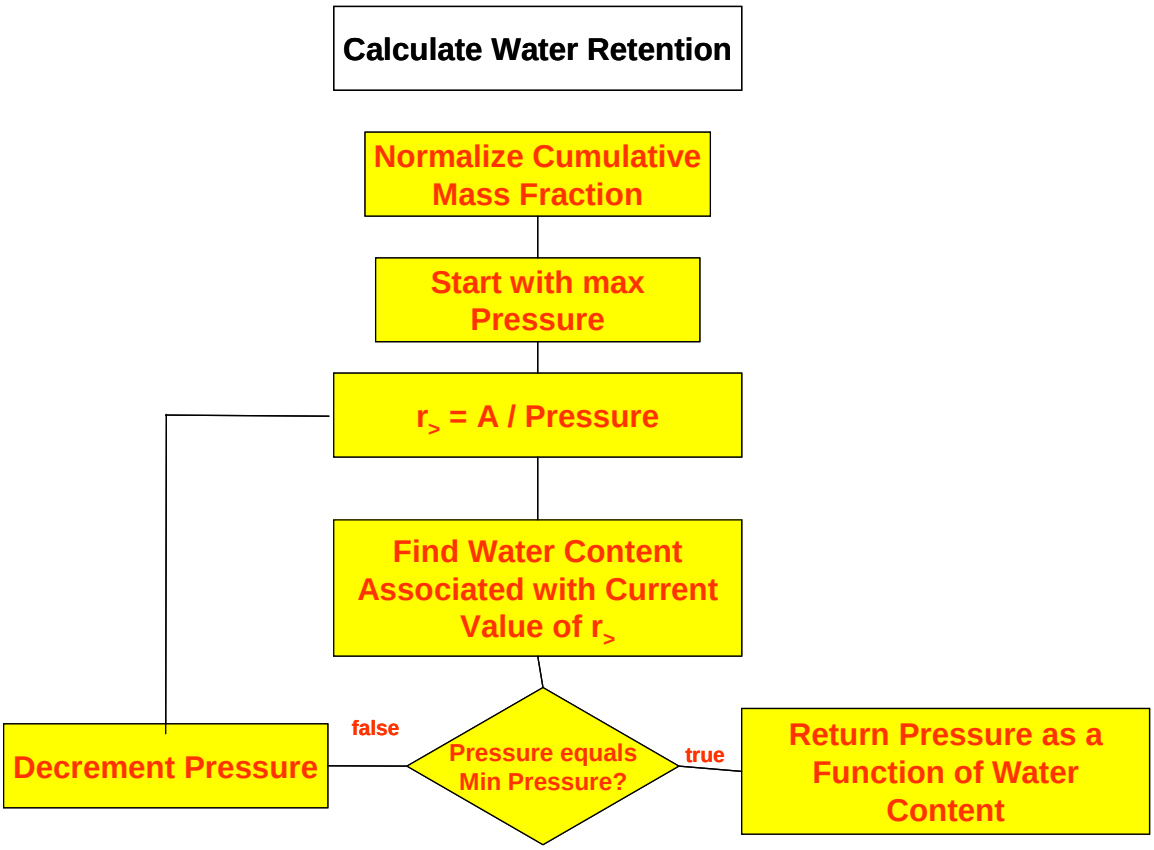

Multiplying the cumulative mass fraction by the porosity normalizes the cumulative mass fraction. This converts it from a variable with values between 0 to 1 to a variable with

values between 0 and φ. We also multiply all the values of the particle size by the proportionality constant of eqn(D1) (here C=0.3) so that we have the pore size distribution. There is no point in using C as an adjustable parameter because any adjustment in C is already accounted for in the adjustable parameter A. The experimental data give the values of the moisture contents at a discrete set of pressure values. The code calculates the moisture contents at these discrete pressure values. Starting with the max pressure, we find the biggest pore size which still contains moisture via eqn(C1). The moisture content associated with this pore size is simply the value of the normalized mass fraction at the same pore size. This is why the cmd is normalized to the porosity, which is equal to the moisture content at full saturation—i.e., the total available pore space (porosity) is filled. We then decrement the pressure, which gives a new value for $r_>$ according to eqn(C1) and repeat the procedure to calculate the moisture content at the new $r_>$, thus building up a table which is representative of the water retention curve. After considering all the provided pressure values, the code returns the predicted curve.

Hydraulic Conductivity

The overview of the hydraulic conductivity code is as follows,

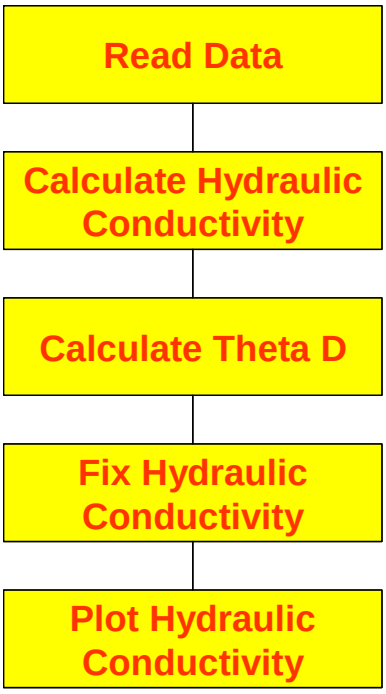

Read Data here scans in a file which contains the cumulative mass fraction as a function of particle size data and the experimental measurements of the hydraulic conductivity as a function of moisture content. There is considerable uncertainty as to whether soils reputed to be saturated (at h=0) are truly saturated. Alternative measurements of the porosity by different means do not provide values consistent with those obtained from water-retention experiments, as noted in the Introduction. One assumption, adopted here, is that this maximum value of the water content given in the data is equal to the porosity. The Calculate Hydraulic Conductivity routine takes as input the cumulative mass fraction as a function of particle size, the porosity, and the critical moisture content for percolation of the soil. Because the McGee Ranch soil is the only soil for which $K(S)$ and water retention are both provided, we take the published value of $\theta_t = 0.108$ (Hunt 2004). It returns the predicted ratio of the hydraulic conductivity as a function of moisture content divided by the hydraulic conductivity at full saturation, $K(\theta)/K_S$, as in eqn(T19), where $K_S = K(S = 1)$.

The predicted hydraulic conductivity will not be valid for moisture contents close to the critical moisture content (see discussion around eqn(T20)). What is needed first is a procedure to determine the value $\theta = \theta_d$ where eqn(T20) supercedes the validity of eqn(T19). This requires implementation of eqn(T22), the new analytical result of this thesis. Therefore, the calculated $K(\theta)$ is fed into the Calculate Theta D routine, which finds θ_d and K_0 as discussed below. For all values of moisture content below the newly-calculated θ_d, we set the hydraulic conductivity equal to eqn. (T20). Finally, the Plot Hydraulic Conductivity routine takes in the predicted and measured hydraulic conductivities and plots them on the same graph.

Breaking down how Calculate Hydraulic Conductivity works we have,

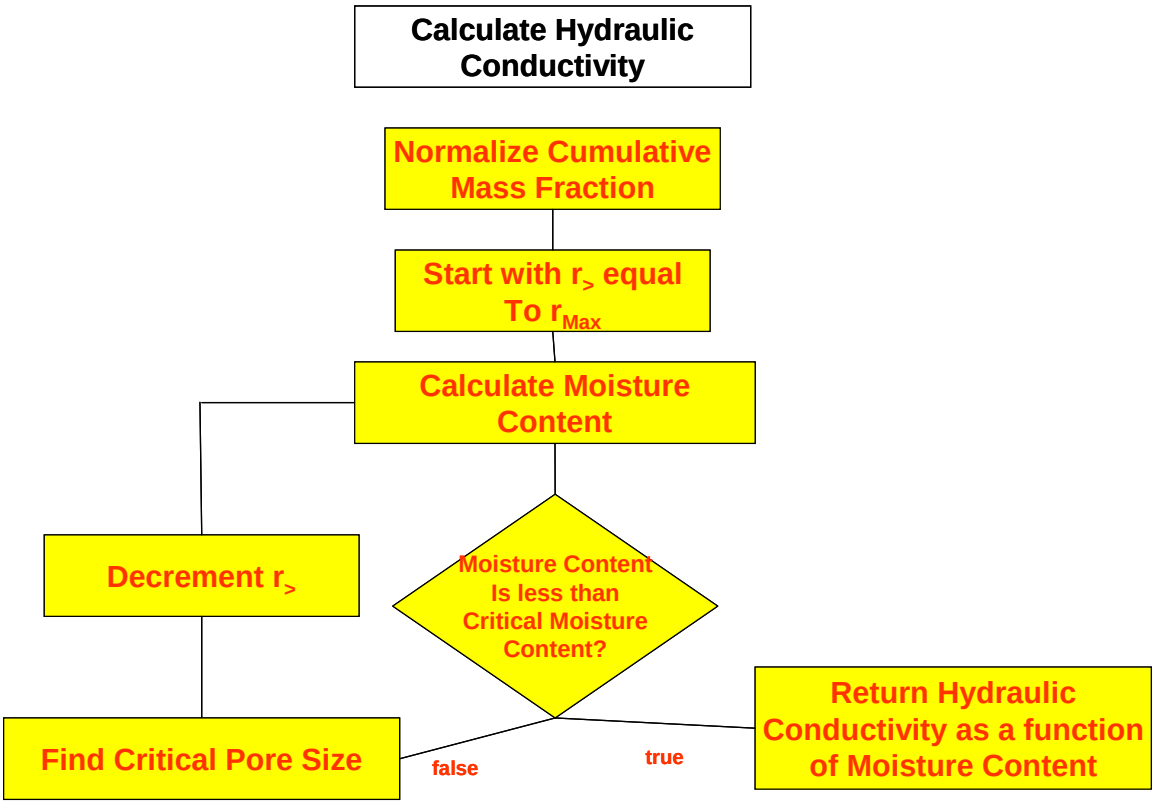

The Normalize Cumulative Mass Fraction routine works the same here as it did for the water retention curves and is not discussed further.

Calculate Hydraulic Conductivity has two principle tasks: to generate θ (in Calculate Moisture Content) and to find K for that θ. Calculate Moisture Content uses $r_>$ as an independent variable to calculate θ while Find Critical Pore Size uses $r_>$ and θ_t to generate r_c. The moisture content of the medium is the sum of contributions from all the pores in the distribution from the smallest up to the largest pore containing moisture. The saturation data have been assumed to be accurate, as discussed above. Since $r_>$ is initially equal to r_m (the largest pore in the medium), and since the largest moisture content reached is the saturated value (equal to the porosity), the first calculation of θ generates φ. We find r_c associated with the current water content, analogously to eqn(T13). Eqn(T13) is the result of integrating eqn(T6) between the limits $r_1=r_c$ and $r_2=r_>$. With the cmd, the analogous sum is performed by taking the value of the normalized cumulative mass (equal to θ) corresponding to $r_>$ and then finding an $r < r_>$ such that the corresponding cumulative mass is $\theta(r_>)-\theta(r)=\theta_t$. The value of r obtained is equal to the critical pore size r_c.

As $r_>$ is decremented each time through the loop, smaller values of the moisture content are obtained. The ratio of $K(\theta)/K_S$ is expressed, similarly to eqn(T19), as the cube of the ratio of $r_c(\theta)/r_c(S=1)$ (shown for the fractal model in eqn(T18)). Find Critical Pore Size starts with the fully saturated case ($\theta=\varphi$) and generates thereby $r_c(S=1)$,. Each time we decrement $r_>$ we find an associated $r_c(\theta=S\varphi)$ and θ. We stop decrementing $r_>$ if the moisture content we just calculated is less than θ_t because the hydraulic conductivity must be zero below θ_t. At this point we exit the loop and cube the ratio of r_c vs $r_c(S=1)$ for all r_c values, which gives the hydraulic conductivity as a function of θ.

The algorithm for the routine which calculates θ_d is as follows,

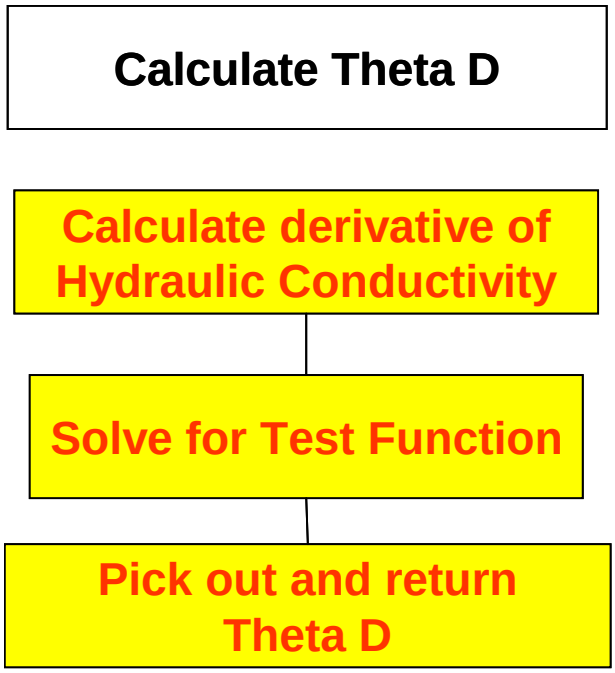

The test function referred to above is obtained from the fundamental new analytic formula of this thesis, eqn(T22). The numerical derivative $dK/d\theta$ is given by the difference in successive K values divided by the difference of successive θ values. Subtracting θ_d from both sides of eqn(T22) leaves on the right hand side an expression (our test function) which is positive or negative depending on whether $K / (dK/d\theta)$ is greater or less than θ_d. We evaluated this test function for all values of $\theta > \theta_t$ and θ_d was chosen to be the value of θ corresponding to the case when the test function most closely approached zero. In the code, this choice is determined by evaluating the sign of the test function. Since the hydraulic conductivity is a positive, monotonically increasing function of moisture content, the value of θ for which our test function goes from negative to positive is the place where it is closest to zero.

Running the Code

For the most part, running the code is pretty simple. The code will easily recognize all the data files if they are in the same folder in which the .m Matlab files are contained. Otherwise, make sure to set up Matlab so that it will look for the data files in whichever folder you wish to store them. If you want to calculate the water retention curve, first you must call the CalculateBestA function. You pass in the number of the data file you which to use (data files are named data#.txt The # is the value you pass into CalculateBestA) as well as a minimum A, maximum A and an increment. The values used for the graphs below are: minimum A = 500, maximum A = 20000 and increment = 50. This function passes back the A value which corresponds to the curve which best fits the measured data based on a least squares estimation. Then all you have to do is call PlotWaterRetention and pass it again the same file number and the *A* value which was returned. If you want to calculate the hydraulic conductivity you only need to make a call to one function, PlotHydraulicConductivity. This simply takes in the file number, a tolerance on how close you want to be to θ_t when finding r_c (currently the code does this iteratively, although an exact solution has recently been suggested by Dr. Skinner) and a value used to decrement $r_>$. The decrement actually applies logarithmically. Initially $r_>$ is equal to r_m*10^0. Each time through the loop the power in the exponent is reduced by the decrement value. The reason for doing this is that we plot the log of the hydraulic conductivity. The values of tolerance and decrement in the graphs below of the hydraulic conductivity were 10^-6 and 10^-2, respectively.

The only other component of running this code successfully is in setting up the data files. Both programs read text files with just a string of numbers. The format for the water retention curves is to have the particle size data, followed by the associated cumulative mass fractions (entered as percents), then the pressure values followed by the

moisture contents. Currently the number of data points for these two functions is 'hard-wired' into the code. In the future you will put the number of data points to be read in directly into the file. The data files for the hydraulic conductivity calculations are formatted again with the particle size data followed by the cumulative mass fraction (in percent), then the experimental data of the hydraulic conductivity which is first values of moisture content followed but their associated hydraulic conductivities.

Results and Comparison with Experiment

The results of the calculation are presented for each soil alongside experimental results for the same soil. This allows an objective evaluation of the effectiveness of the theory and code.

Data relevant to flow in the U.S. Department of Energy Hanford site have been obtained from two sources: 1) An internal Pacific Northwest National Laboratory (PNNL) Report from 1988, (Rockhold et al., 1988) which contains particle size data for eleven samples of the McGee Ranch soil, as well as experimental water-retention curves and the hydraulic conductivity as a function of saturation for 5 different depths. 2) A second internal PNNL report (Vadose Zone Transport Study) with data supplied electronically by Dr. Mark Rockhold in 2005. This latter collection contains the particle-size data and water-retention curves of 53 soils, as well as the saturated hydraulic conductivity.

Using data set 1 it is possible to validate theory and code for the hydraulic conductivity and for the water retention curves, but using data set 2 it is possible only to validate the coded predictions for the water-retention curves. Using data set 2, however, which is taken from a site believed to be analogous to the location of the Technetium spill (Ward et al., 2006), it is possible to predict the hydraulic conductivities of the medium constituents at interfacial tensions similar to what is typically observed at the BC Crib site. While such predictions cannot at this time be verified, they may be useful for risk analysis of this spill.

In the case of the water-retention curves, one parameter, A, must be fit to experiment in order to allow a reasonable evaluation of the accuracy of the procedure. This parameter describes the relationship between the air-water interfacial tension and the radius of the pore. Equivalently, one may choose a minimum suction pressure at which air will enter the system, though in this particular case some confusion exists due to the fact that the pressure at which air can enter the largest pores is not the same pressure at which air enters the system. Such pores must also form an interconnected, percolating network for air actually to enter the system. In any case, the fitted values of the parameter A have been tabulated (Table 1) for the 53 (7 of the 60 data sets were missing water retention data) Vadose Transport Field Study soils along with the characteristics of the soils. The least squares fits for comparison of prediction and experiment then yield the residuals in Table (1) under the column labeled 'Fit'. The only use for the number given by the least squares residuals is that it tells us how close the prediction matches the experimental data. Due to a lack of uncertainty in the data, we have no way of quantifying whether the theory actually falls within the error bars of the data.

Table 1

Data Set	A	Fit	Soil characteristics
1	13600	0.047324	Disturbed (ring filled by hand) contains plant roots, medium coarse
2	5000	0.049297	Disturbed (ring filled by hand) contains plant roots, medium coarse/coarse
3	11200	0.070225	undisturbed, wet, coarse sand
4	5800	0.085624	undisturbed/disturbed , wet, coarse sand, subsample rose in the ring
5	4200	0.107021	undisturbed, wet, coarse sand
6	8300	0.07337	undisturbed, wet, coarse sand
7	-1	-1	undisturbed, wet, (medium) coarse sand
8	5800	0.106359	undisturbed, coarse sand/almost gravel
9	5800	0.055963	Disturbed (ring filled by hand). Obtained only a small amount of grab sample
10	4100	0.079513	undisturbed, coarse sand/almost gravel, dry
11	4200	0.053685	undisturbed, coarse sand
12	4100	0.08498	undisturbed, coarse sand

13	3100	0.055784	undisturbed, medium coarse/coarse sand
14	3500	0.069439	undisturbed, medium coarse/coarse sand
15	4900	0.060298	undisturbed, medium coarse sand
16	3100	0.062378	undisturbed, medium coarse sand
17	3100	0.077423	undisturbed, medium coarse sand
18	6800	0.049528	undisturbed, medium coarse sand
19	5000	0.049068	undisturbed, medium coarse sand
20	4200	0.078984	undisturbed, fine/medium coarse sand/coarse sand
21	11600	0.097672	undisturbed, coarse sand/almost gravel, fine at bottom
22	5800	0.091046	undisturbed, coarse sand(almost gravel)
23	6100	0.052222	undisturbed, coarse sand(almost gravel)
24	5800	0.098742	undisturbed, coarse sand
25	-1	-1	undisturbed, coarse sand at top, fine at bottom
26	3100	0.164148	undisturbed, fine sand
27	8400	0.114908	undisturbed, fine sand at top, coarse at bottom, wet
28	-1	-1	extra subsample of 26 (S-1/42D), probably pretty disturbed.
29	-1	-1	extra subsample of 25 (S-1/42C), probably pretty disturbed.
30	-1	-1	(un)disturbed, coarse sand
31	8300	0.040095	(un)disturbed, fine sand at top, coarse at bottom, wet
32	4200	0.050044	(un)disturbed, coarse sand dry
33	3100	0.053629	(un)disturbed, coarse sand dry
34	5800	0.081888	undisturbed 0.9 cm high damp, loose
35	4300	0.039622	undisturbed 0.9 cm high damp
36	8100	0.063754	undisturbed 1.2 cm high wet semi solid
37	-1	-1	undisturbed 1.5 cm high damp
38	5800	0.034589	undisturbed 1.4 cm high damp
39	8300	0.034493	disturbed finer cemented
40	4100	0.052255	undisturbed 1.2 cm high
41	5800	0.049818	semi undisturbed fine, cemented
42	5800	0.071255	0.6 cm high coarse dry
43	6100	16611.81	level coarse loose damp
44	16600	0.08505	level coarse damp
45	5800	0.069741	0.3 cm very dry loose
46	3100	0.0589	0.8 cm damp loose
47	3800	0.058455	0.9 cm damp loose
48	4300	0.060818	0.4 cm fines & sand damp
49	5800	0.103919	0.6 cm damp coarse
50	3800	0.05805	damp coarse
51	8300	0.066216	1.1 cm damp fine cemented
52	5800	0.090962	damp medium fine sand
53	4100	0.057782	1.3 cm high damp loose
54	5000	0.077663	0.5 cm high some silt, damp loose
55	5000	0.038078	1.1 cm high damp loose some silt
56	10000	0.064537	0.9 cm wet silt, compacted
57	9700	0.034712	0.7 cm damp silt sand
58	-1	-1	0.6 cm dry loose average sand
59	4000	0.070959	level very dry loose
60	3800	0.049201	level damp loose sand

Table two summarizes how much of the soil consisted of particles within a given size range, as well as porosity of the sample. Gravel includes particles larger than 2mm, Sand 0.05mm-2mm, Silt 0.002mm-0.05mm and Clay particles are smaller than .002mm. The porosity values of some of the samples were not available.

Table 2

Data Set	Gravel Weight %	Sand Weight %	Silt Weight %	Clay Weight %	Porosity cm3/cm3
1	4.36	81.24	10.66	3.75	0.376
2	1.95	94.74	2.06	1.25	0.422
3	1.47	88.33	7.70	2.50	0.389
4	0.33	93.83	3.34	2.50	0.400
5	0.25	97.71	0.79	1.25	0.418
6	0.18	92.32	5.00	2.50	0.399
7	0.32	91.30	5.88	2.50	
8	0.14	84.76	11.35	3.75	0.388
9	0.77	88.67	6.81	3.75	0.464
10	0.27	98.48	0.00	1.25	0.452
11	0.63	98.12	0.00	1.25	0.463
12	1.37	96.13	1.25	1.25	0.464
13	0.74	98.01	0.00	1.25	0.427
14	0.40	97.10	1.25	1.25	0.452
15	0.38	89.07	8.06	2.50	0.379
16	0.59	96.91	1.25	1.25	0.433
17	0.17	97.33	1.25	1.25	0.451
18	0.54	88.55	7.16	3.75	0.369
19	0.21	93.16	5.38	1.25	0.397
20	0.00	90.21	6.04	3.75	0.474
21	3.80	90.10	3.60	2.50	0.359
22	0.94	94.27	2.30	2.50	0.391
23	1.28	96.22	0.00	2.50	0.404
24	0.43	89.85	5.97	3.75	0.374
25	0.43	93.54	3.53	2.50	
26	0.28	74.23	21.75	3.75	0.403
27	0.15	90.02	6.08	3.75	0.384
28	3.22	76.11	15.67	5.00	
29	1.72	85.77	8.76	3.75	
30	2.00	85.49	8.76	3.75	
31	0.14	82.15	11.46	6.25	0.360
32	0.41	97.09	0.00	2.50	0.424
33	0.00	95.24	1.01	3.75	0.445
34	0.00	92.67	3.58	3.75	0.403
35	1.69	90.81	3.75	3.75	0.423

36	1.21	85.29	7.25	6.25	0.382
37	4.46	90.54	1.25	3.75	
38	1.18	82.70	9.87	6.25	0.386
39	2.46	78.89	12.41	6.25	0.374
40	0.07	88.17	6.76	5.00	0.456
41	0.54	72.65	21.93	4.88	0.356
42	0.73	87.51	8.01	3.75	0.406
43	0.31	85.25	10.69	3.75	0.410
44	1.14	89.36	7.00	2.50	0.401
45	0.84	85.61	9.80	3.75	0.430
46	0.78	91.96	2.26	5.00	0.421
47	1.92	90.58	2.50	5.00	0.430
48	2.99	92.01	1.25	3.75	0.429
49	1.79	90.95	4.76	2.50	0.392
50	0.08	94.93	2.50	2.50	0.431
51	0.96	84.19	9.86	5.00	0.360
52	1.23	85.19	8.59	5.00	0.360
53	0.35	95.90	1.25	2.50	0.448
54	0.37	84.78	9.86	5.00	0.411
55	0.00	87.68	7.32	5.00	0.453
56	0.61	84.65	11.00	3.75	0.368
57	0.56	74.64	17.31	7.50	0.354
58	2.23	91.52	3.75	2.50	
59	0.19	92.62	3.43	3.75	0.424
60	0.00	92.50	3.75	3.75	0.415

The figures R1 through R20 show twenty of the fifty-three water retention predictions for the soil data received from the Hanford site. These predictions (the dashed lines) are plotted along side the experimentally determined curves (the solid lines) provided in the data. In the title of the figures, information is provided to show: what data set is evaluated, the value of *A* which fits the prediction to the data best (as calculated by the least squares routine) and a value called 'Fit' which is the sum of the least squares residuals divided by the number of residuals. Due to the absence of any knowledge of the error in our data, we are unable to determine conclusively that our model fits the experiment. This fit value only tells us which choice of *A* causes our prediction to fit best with the experimental data provided, relative to all other choices of *A*.

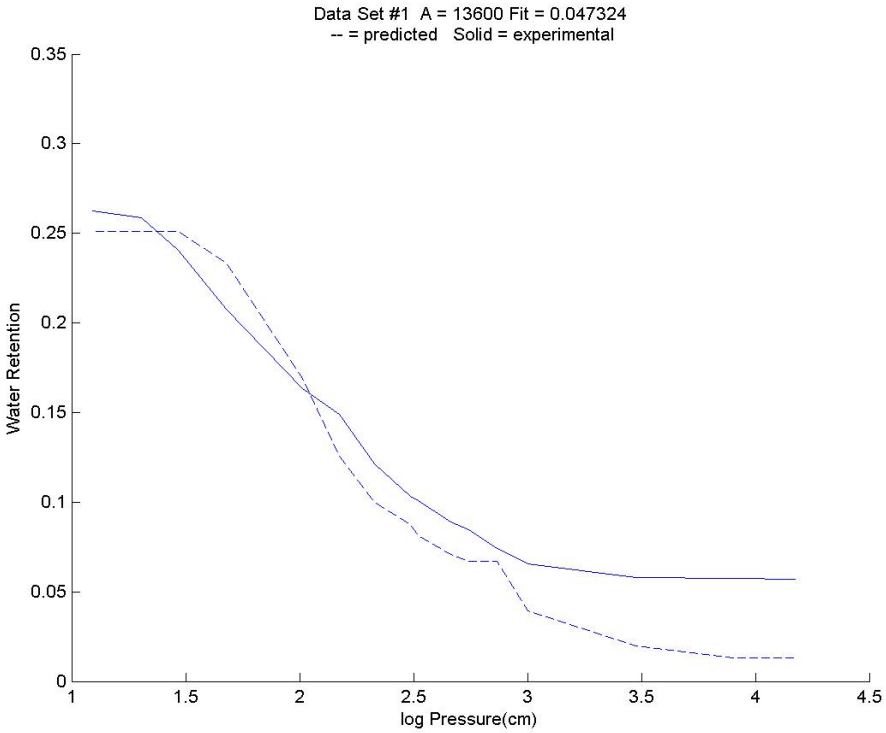
Data Set #1 A = 13600 Fit = 0.047324
-- = predicted Solid = experimental
Water Retention
log Pressure(cm)
0.35
0.3
0.25
0.2
0.15
0.1
0.05
0
1
1.5
2
2.5
3
3.5
4
4.5

Fig R1

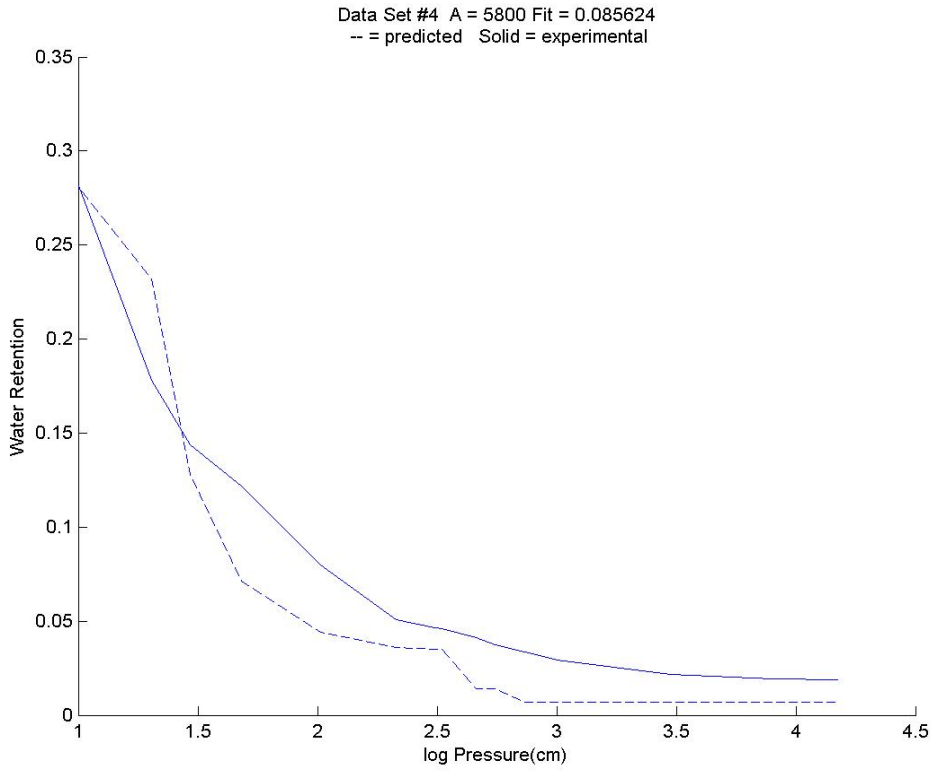
Data Set #4 A = 5800 Fit = 0.085624
-- = predicted Solid = experimental
Water Retention
log Pressure(cm)
0.35
0.3
0.25
0.2
0.15
0.1
0.05
0
1
1.5
2
2.5
3
3.5
4
4.5

Fig R2

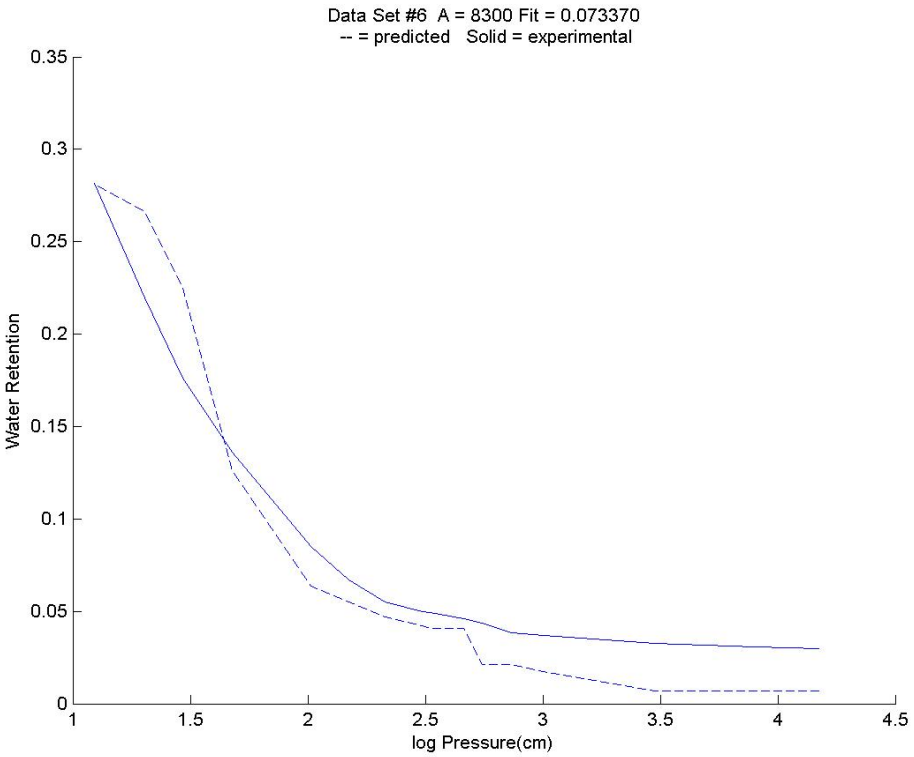
Data Set #6 A = 8300 Fit = 0.073370
-- = predicted Solid = experimental
Water Retention
log Pressure(cm)
0.35
0.3
0.25
0.2
0.15
0.1
0.05
0
1
1.5
2
2.5
3
3.5
4
4.5

Fig R3

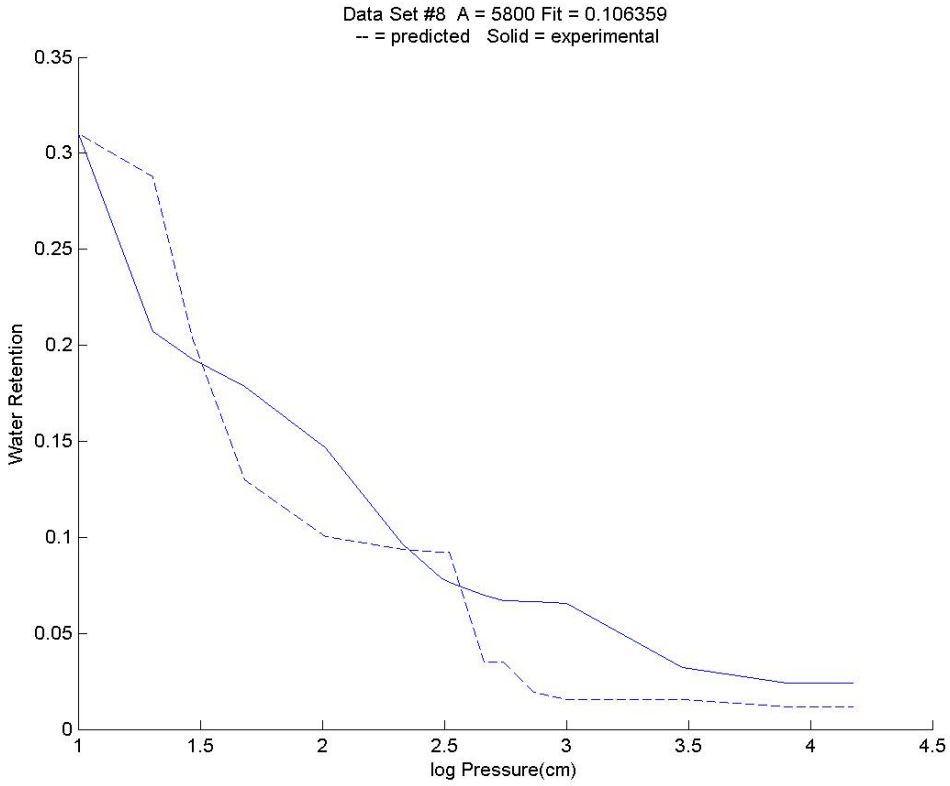
Data Set #8 A = 5800 Fit = 0.106359
-- = predicted Solid = experimental
Water Retention
log Pressure(cm)
0.35
0.3
0.25
0.2
0.15
0.1
0.05
0
1
1.5
2
2.5
3
3.5
4
4.5

Fig R4

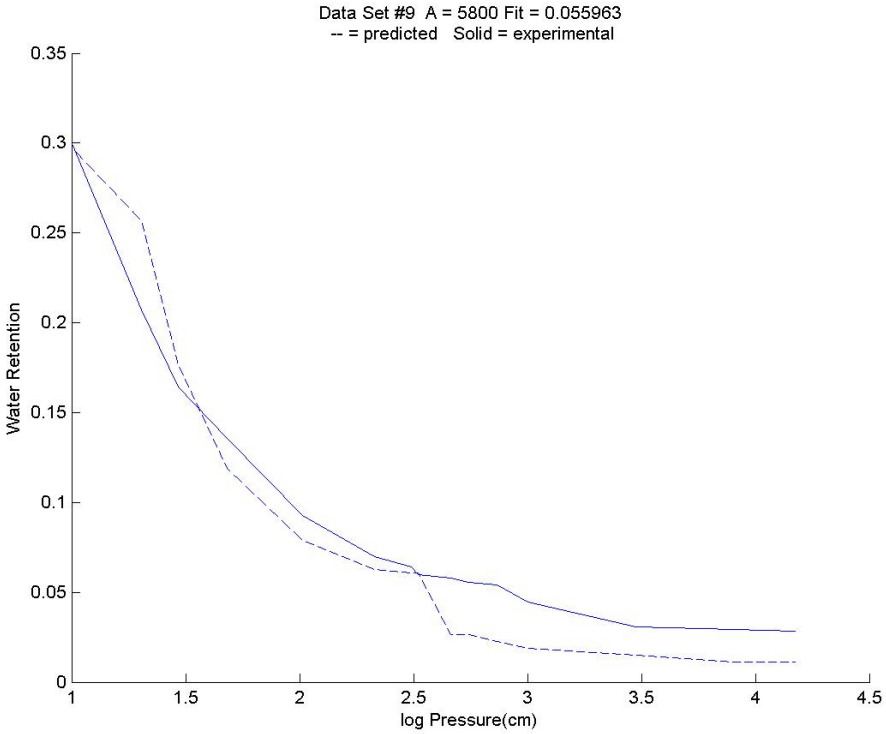
Data Set #9 A = 5800 Fit = 0.055963
-- = predicted Solid = experimental
Water Retention
log Pressure(cm)
0.35
0.3
0.25
0.2
0.15
0.1
0.05
0
1
1.5
2
2.5
3
3.5
4
4.5

Fig R5

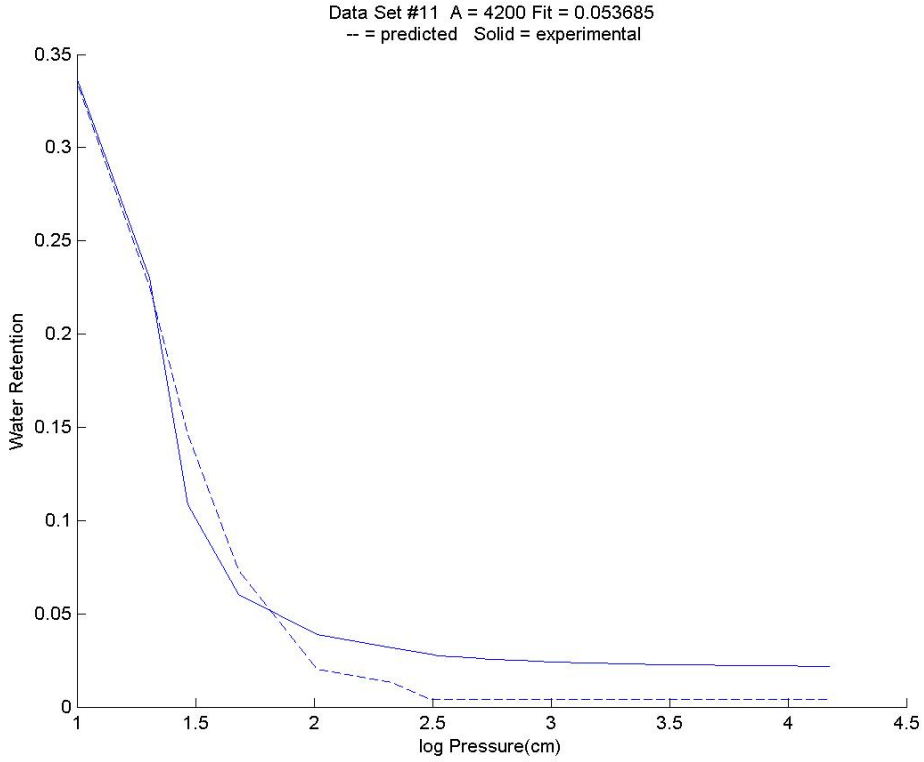
Data Set #11 A = 4200 Fit = 0.053685
-- = predicted Solid = experimental
Water Retention
log Pressure(cm)
0.35
0.3
0.25
0.2
0.15
0.1
0.05
0
1
1.5
2
2.5
3
3.5
4
4.5

Fig R6

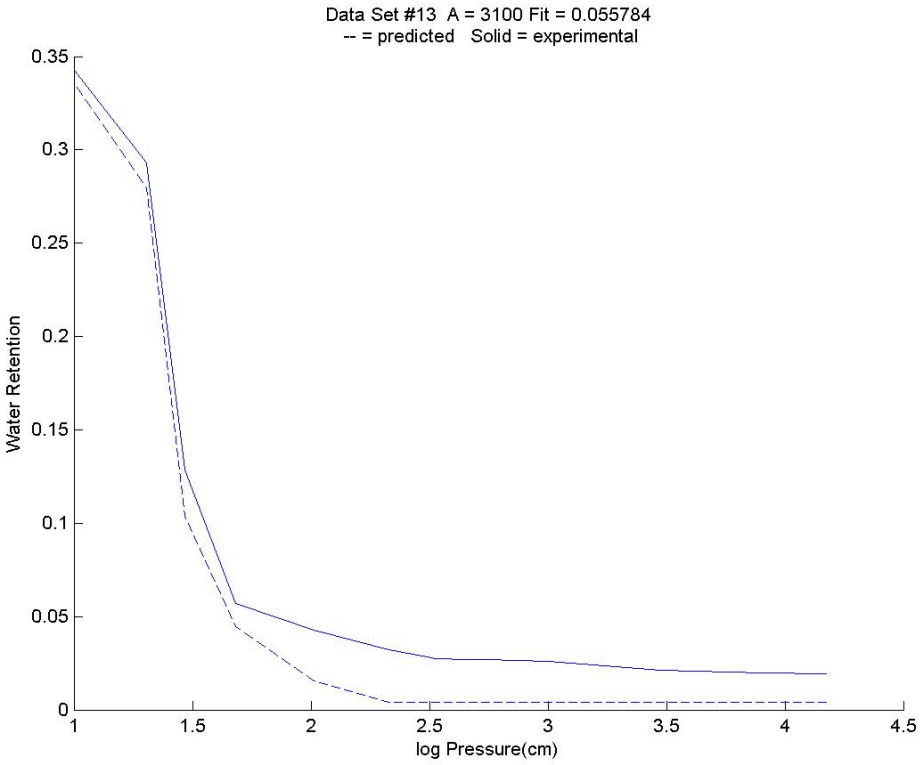
Data Set #13 A = 3100 Fit = 0.055784
-- = predicted Solid = experimental
Water Retention
log Pressure(cm)
0.35
0.3
0.25
0.2
0.15
0.1
0.05
0
1
1.5
2
2.5
3
3.5
4
4.5

Fig R7

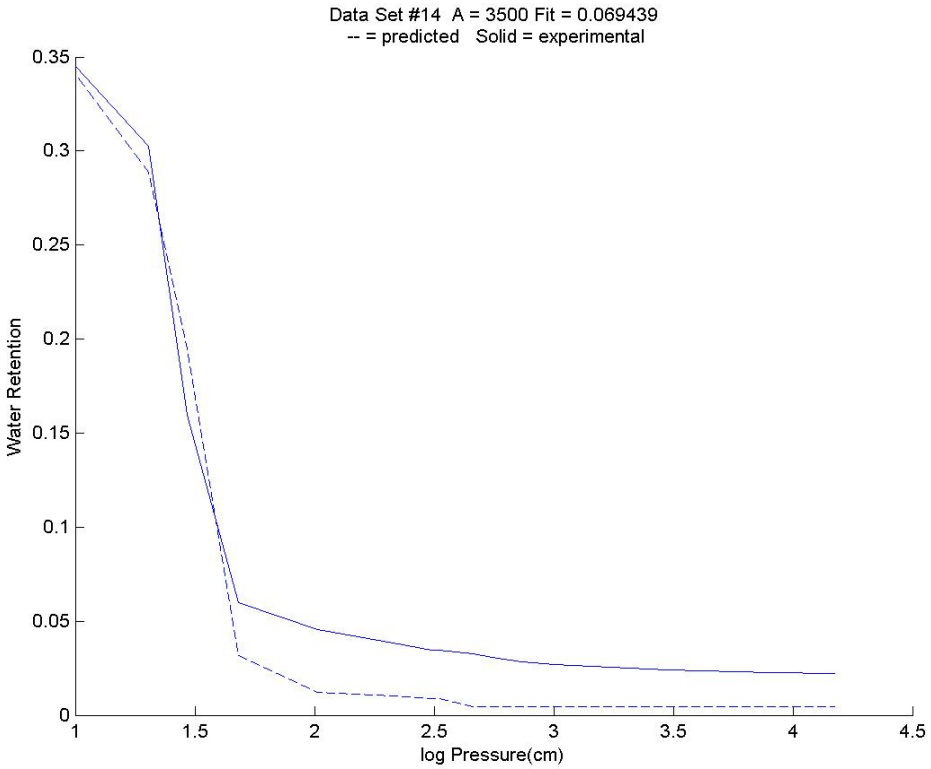
Data Set #14 A = 3500 Fit = 0.069439
-- = predicted Solid = experimental
Water Retention
log Pressure(cm)
0.35
0.3
0.25
0.2
0.15
0.1
0.05
0
1
1.5
2
2.5
3
3.5
4
4.5

Fig R8

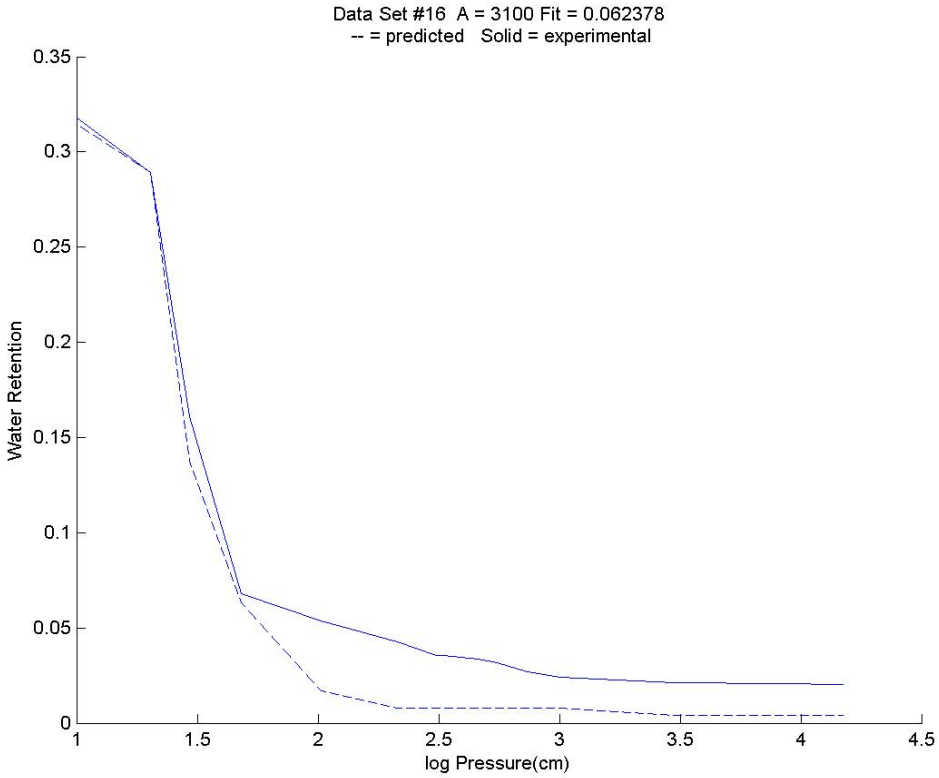

Fig R9

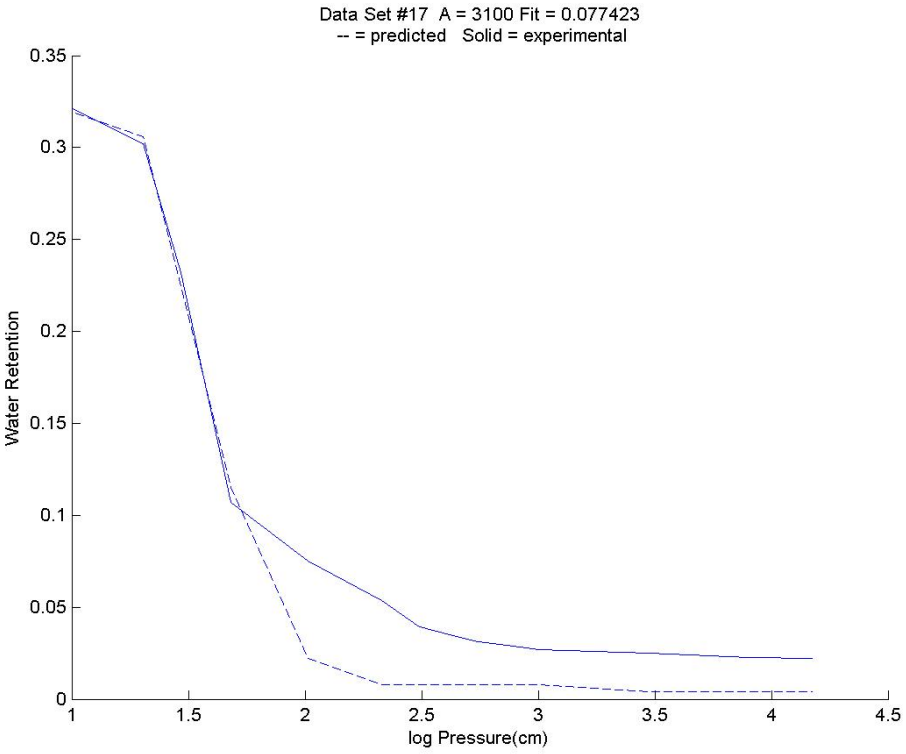

Fig R10

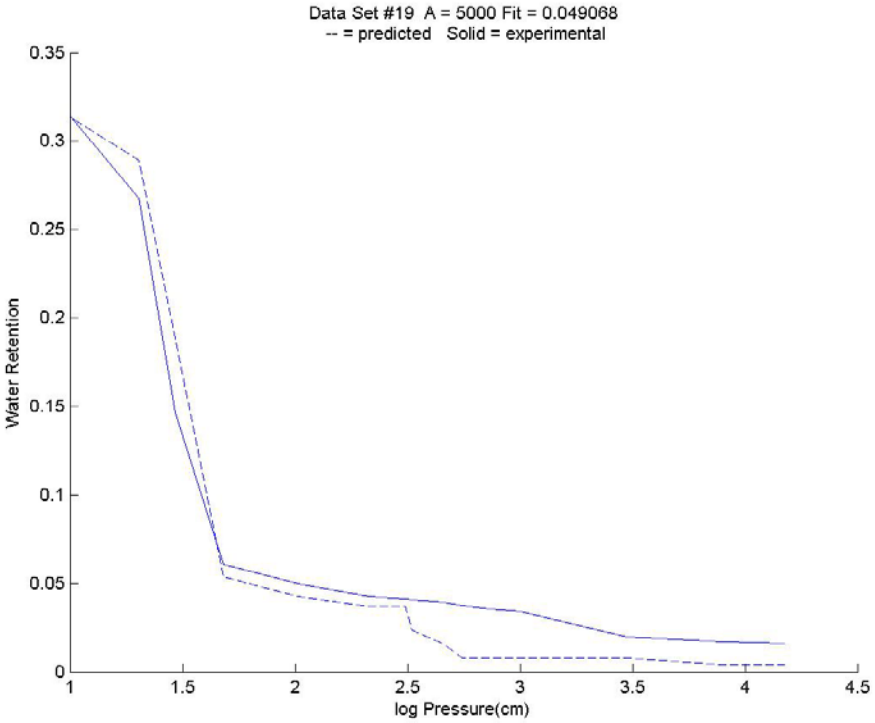

Fig R11

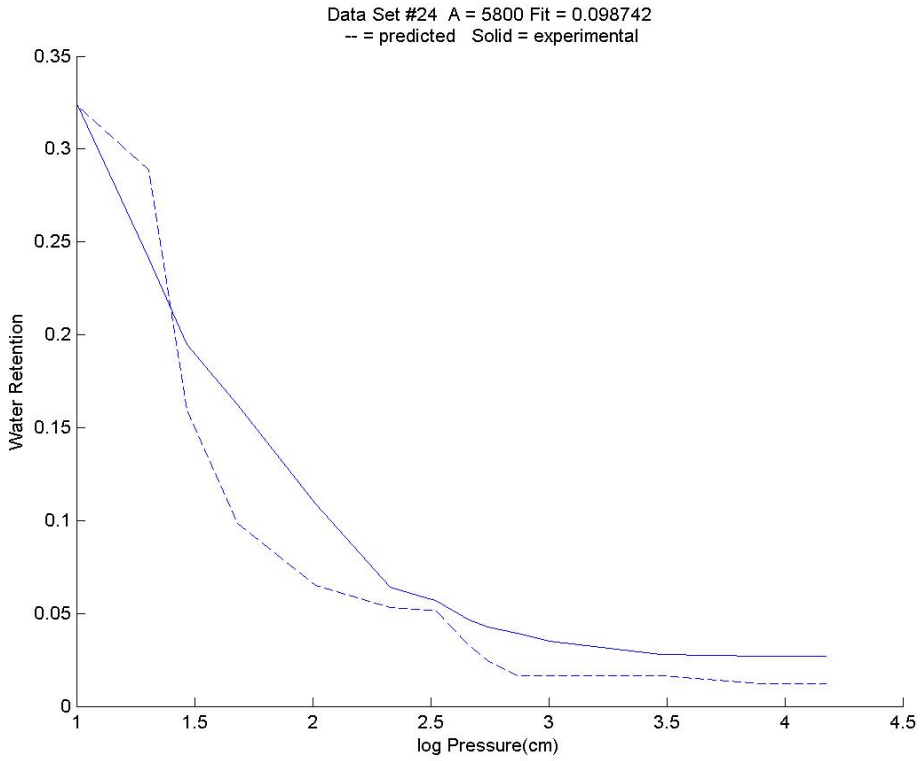

Fig R12

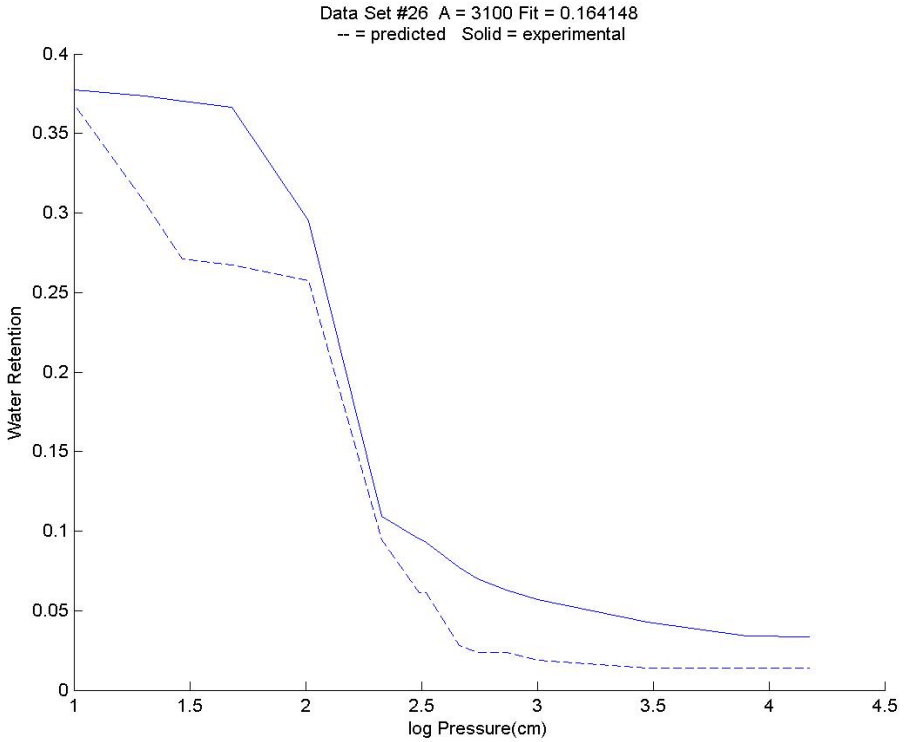

Fig R13

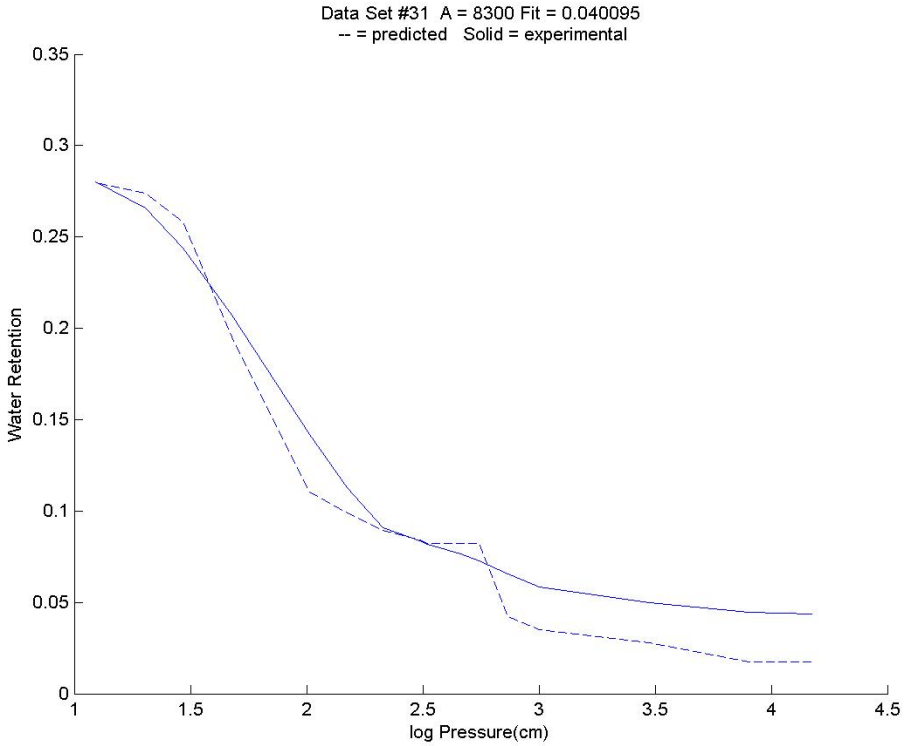

Fig R14

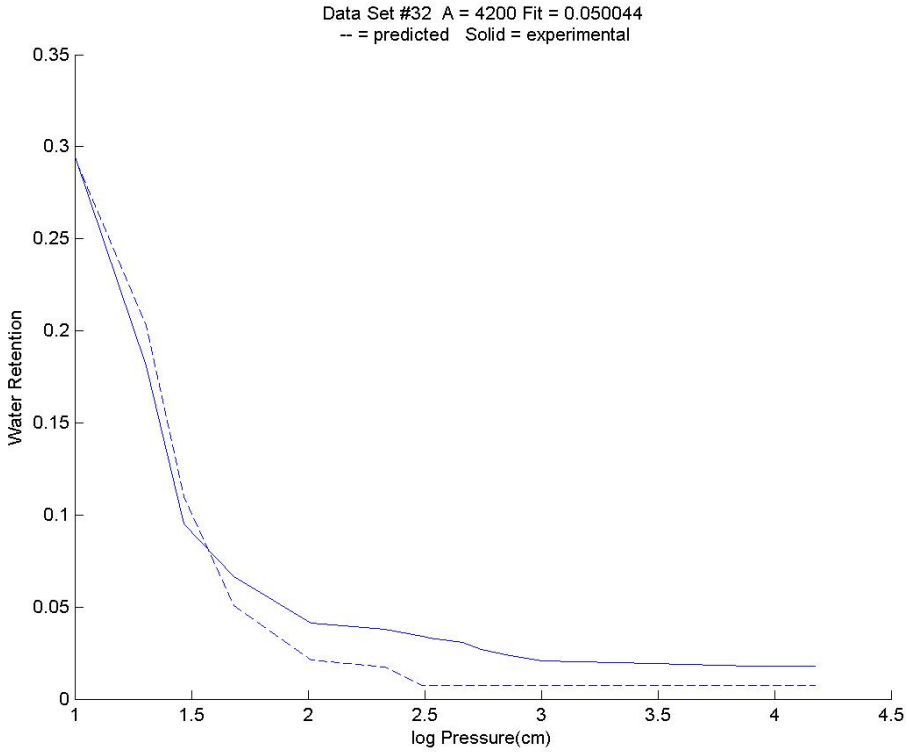

Fig R15

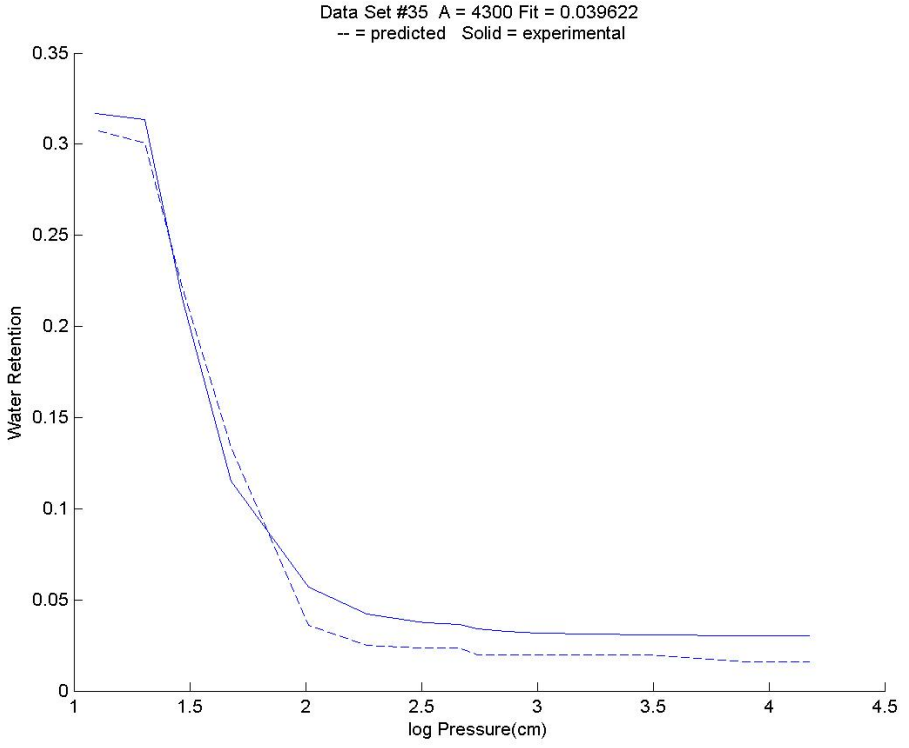

Fig R16

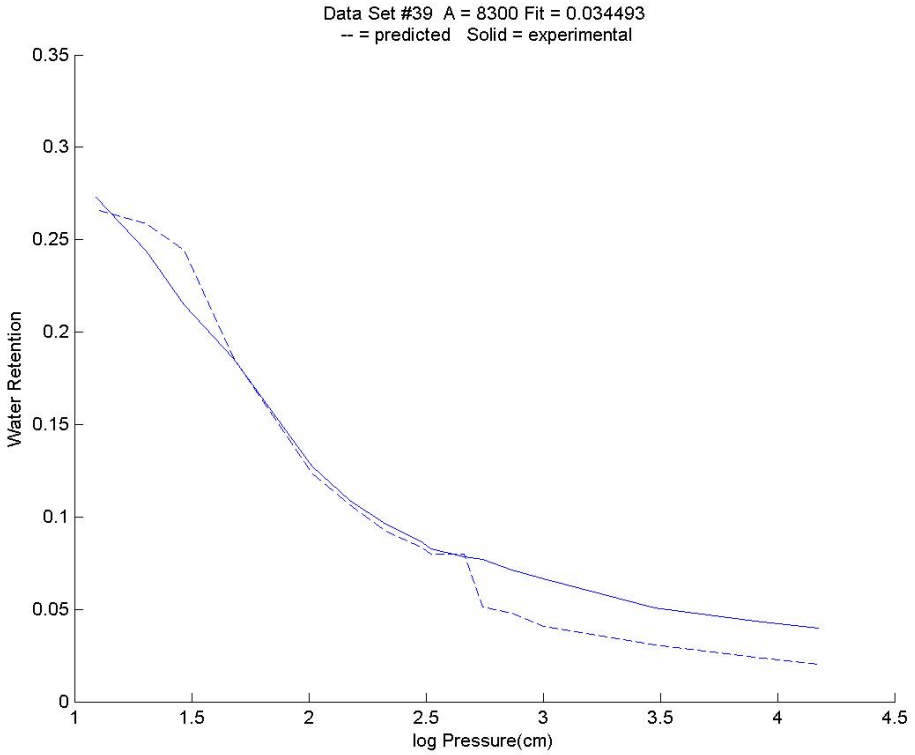

Fig R17

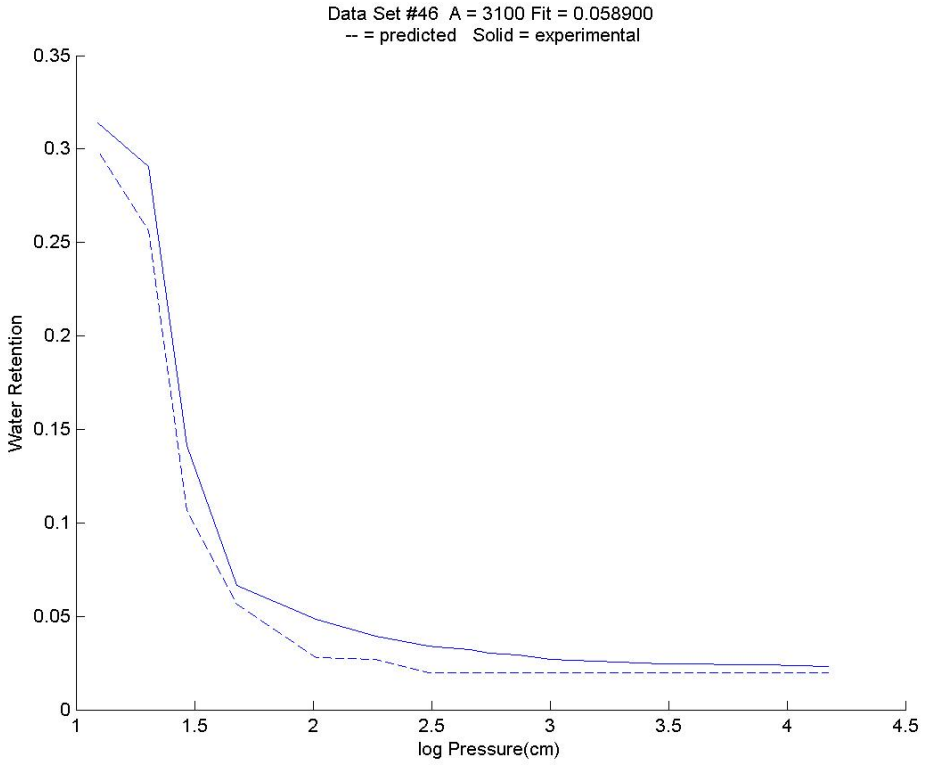

Fig R18

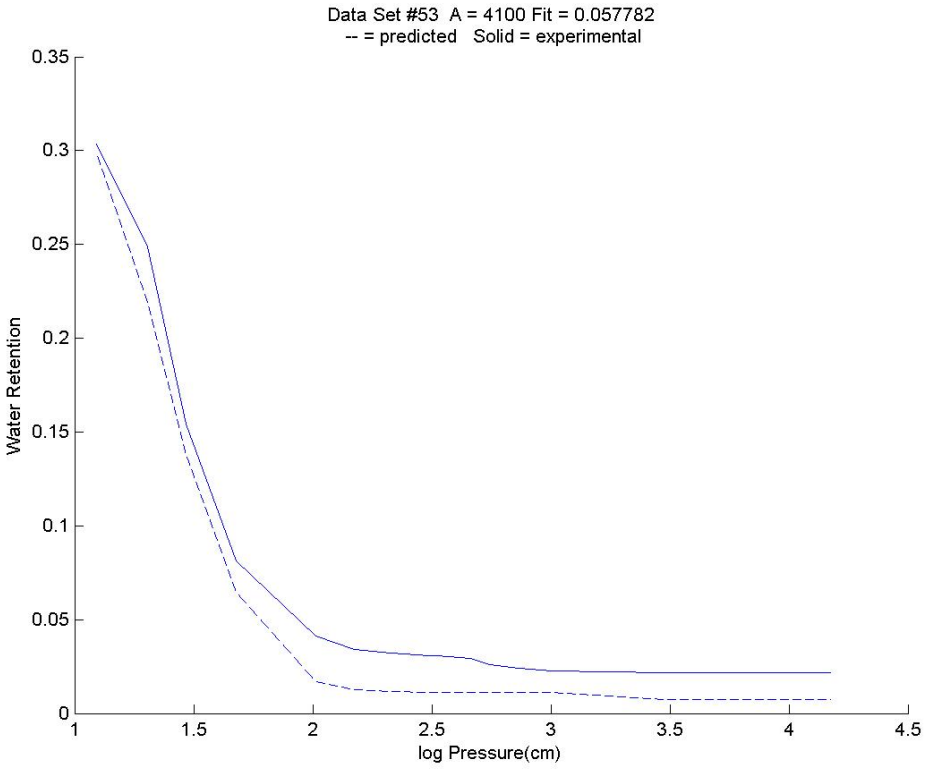

Fig R19

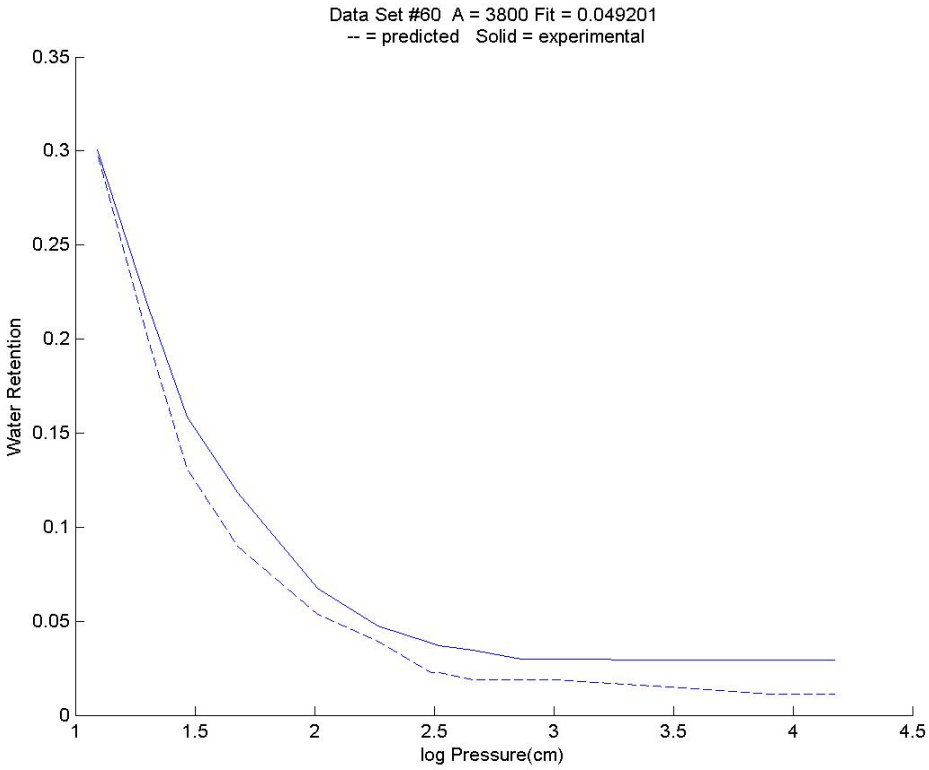

Fig R20

When we consider the comparison of predicted and observed water retention curves we find that most yield satisfactory agreement if the water content is not too low. For lower water contents we expect the predicted water content to lie below the actual value because of the cross-over in K to the percolation power-law, which leads to very low values of the hydraulic conductivity. The reason is that with k values of 10-8cm/s or smaller, the drying of a soil will typically take years or longer—experimental time scales which are never approached. This particular situation was already investigated in detail, though only for the specific fractal model, by Hunt and Skinner (2005). Nevertheless the general conclusions still apply here.

Comparisons of predicted and experimental values of the hydraulic conductivity are given in the set of figures Fig R21-R31. The experimental data for both the particle sizes and the hydraulic conductivity were obtained from McGee Ranch (Rockhold et al., 1988). Particle-size data were taken for eleven soil samples near the surface, while hydraulic conductivity measurements were taken at five different depths. It is not clear which K measurements correspond to which particle-size data sets. As a consequence, I decided to investigate the predictions resulting from all 11 psd's for each of the five K/Ks measurements separately. Even though predictions for each of the eleven soils were thus compared to all five measurements of K, I only display the experimental K which agrees best with the prediction. The number corresponding to a particular soil sample is provided in the title as well as which hydraulic conductivity curve is plotted. A further inquiry was made into the relevance of the particular choice of the discretization in the distributions, i.e., the influence of the finite widths of the bins (see Data section). The solid line represents the experimental data. The two alternate predictions are shown as the

dotted and dashed lines and the "goodness" of the fit is again described by the residuals of sum of the squares of the deviations.

The dotted line corresponds to the interpretation in the cumulative mass fraction that R_1 is the smallest particle in the sample. The dashed line corresponds to the interpretation that the smallest particle in the sample has zero radius. Each of the dotted and dashed lines has its own 'Fit' value, which represents the value returned from the least squares routine. Again, this value gives us no information as to how well our model fit the data. It just tells us which of our predictions are closest to the data provided us. These values are all summarized in table(3). It appears that there is, in the present case, no meaningful difference between the two discretization procedures.

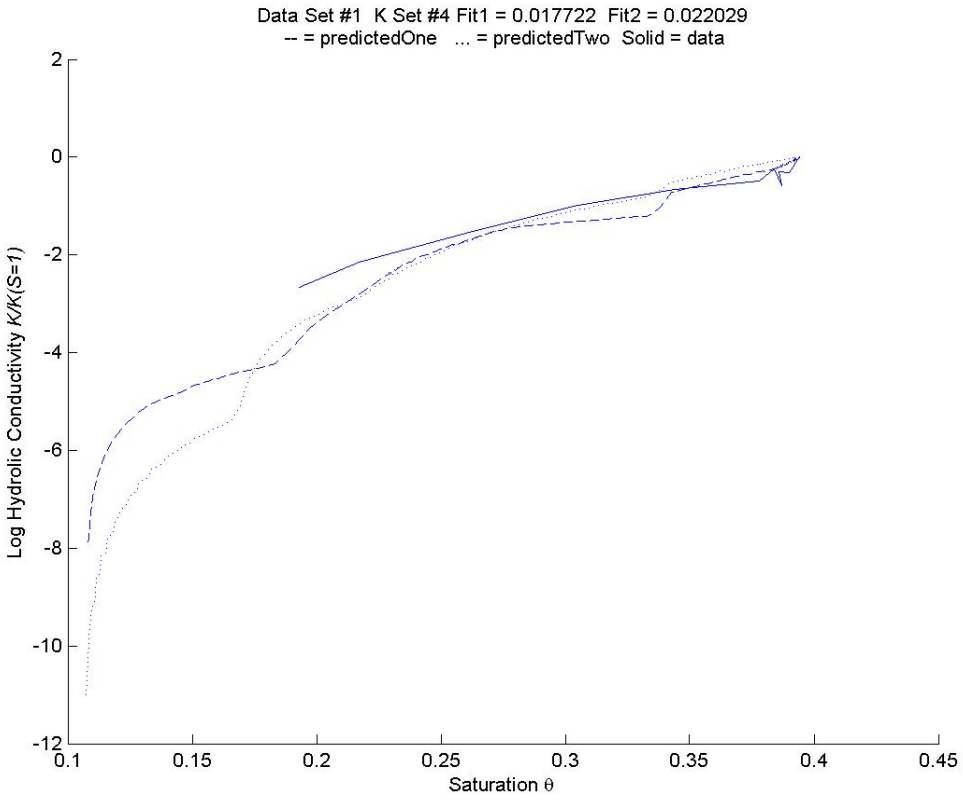

Fig R21

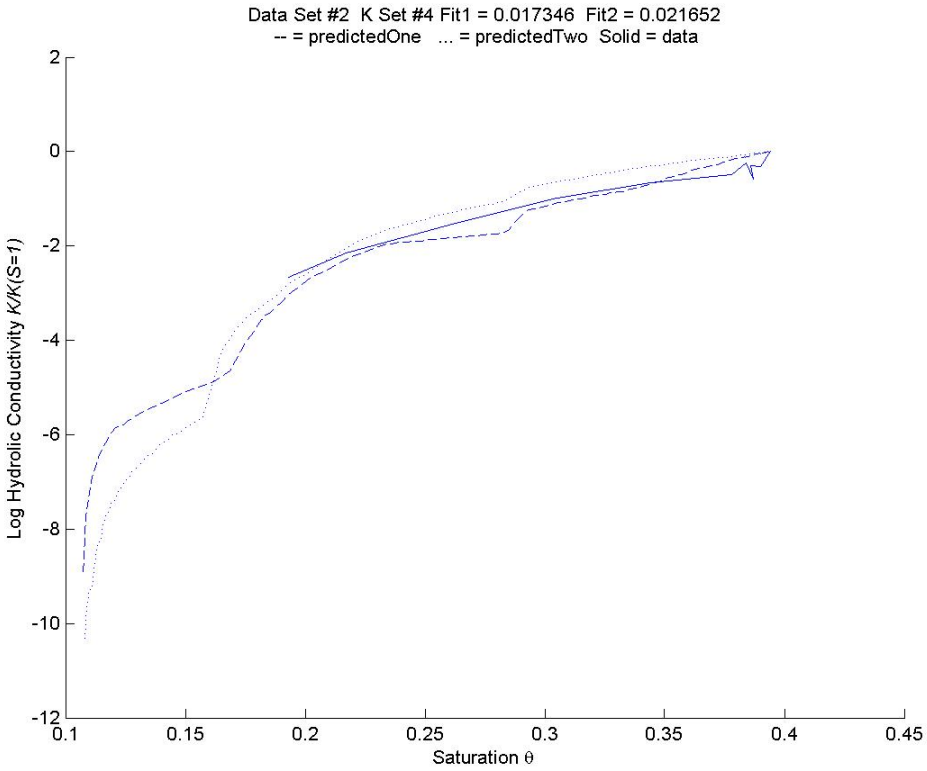

Fig R22

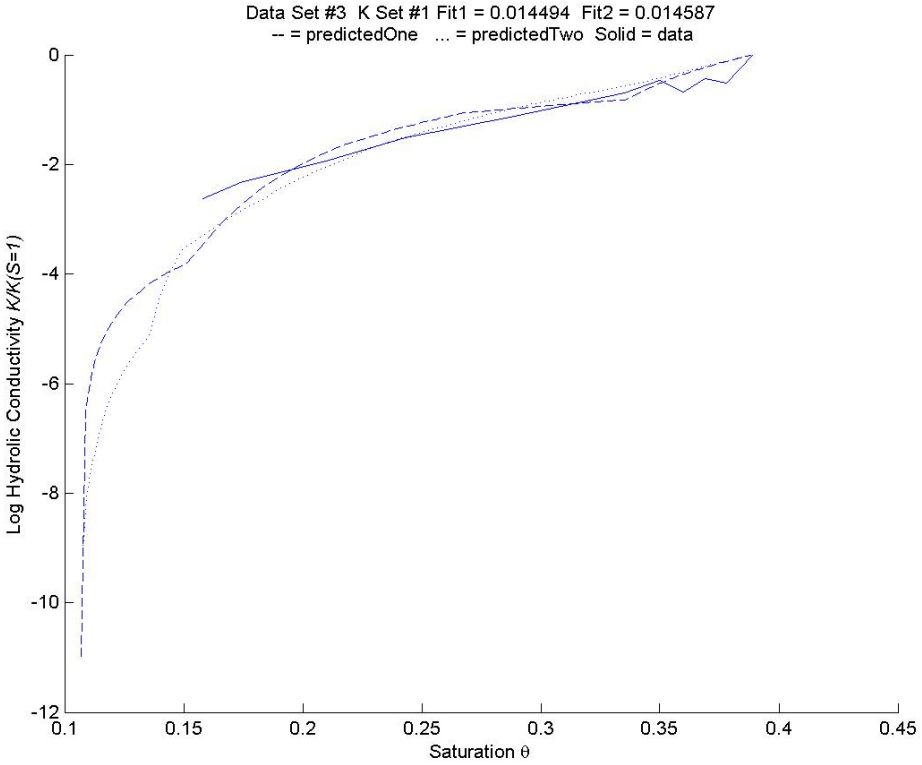

Fig R23

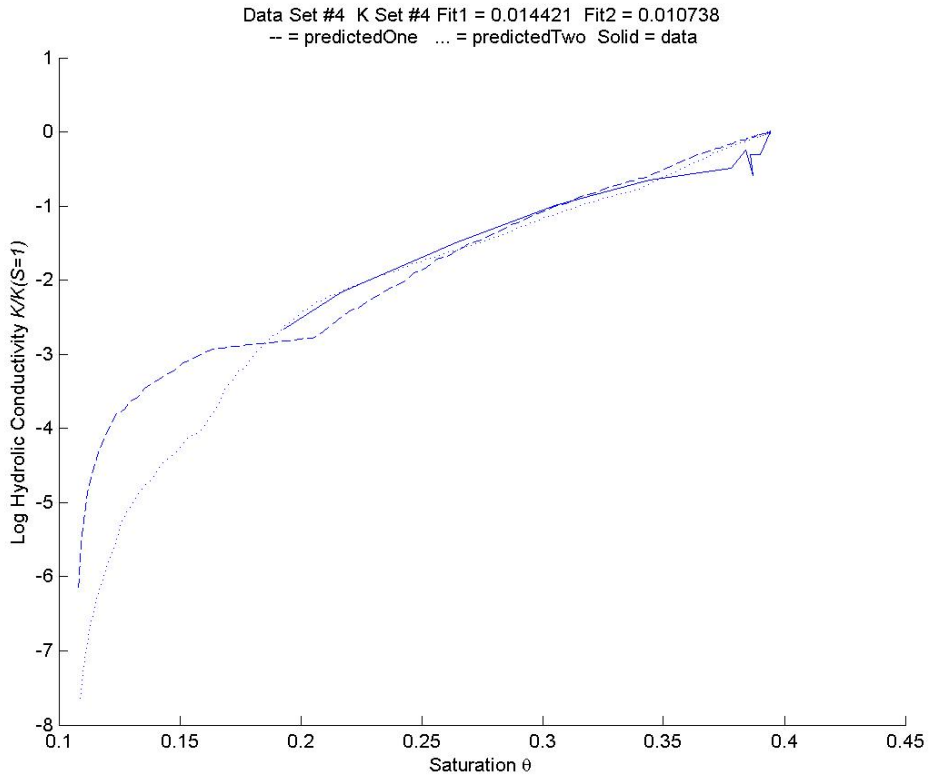

Fig R24

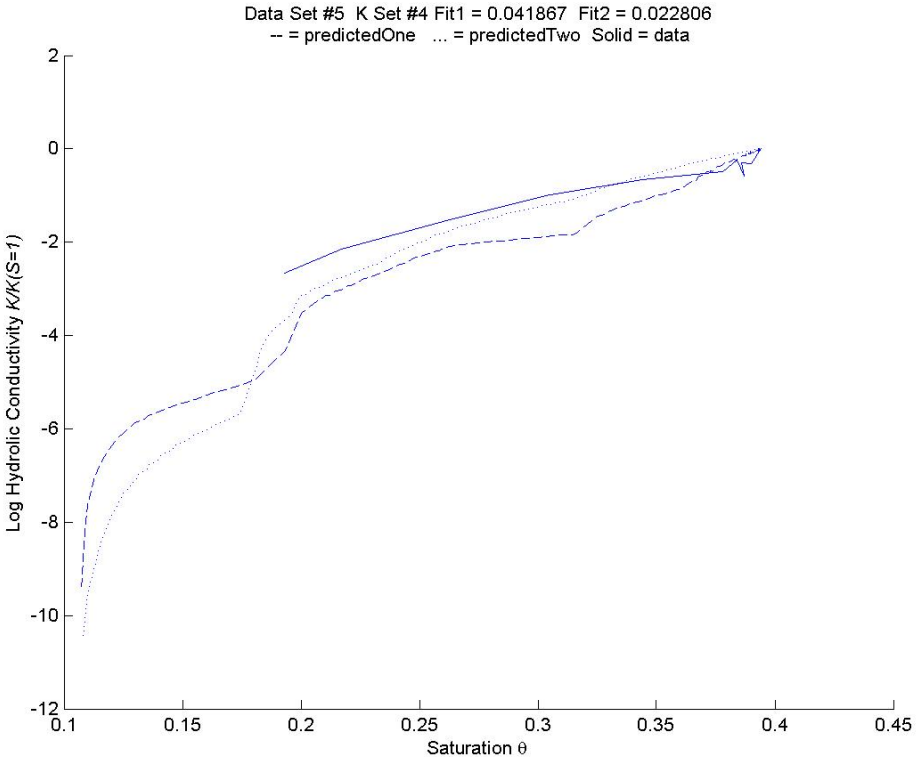

Fig R25

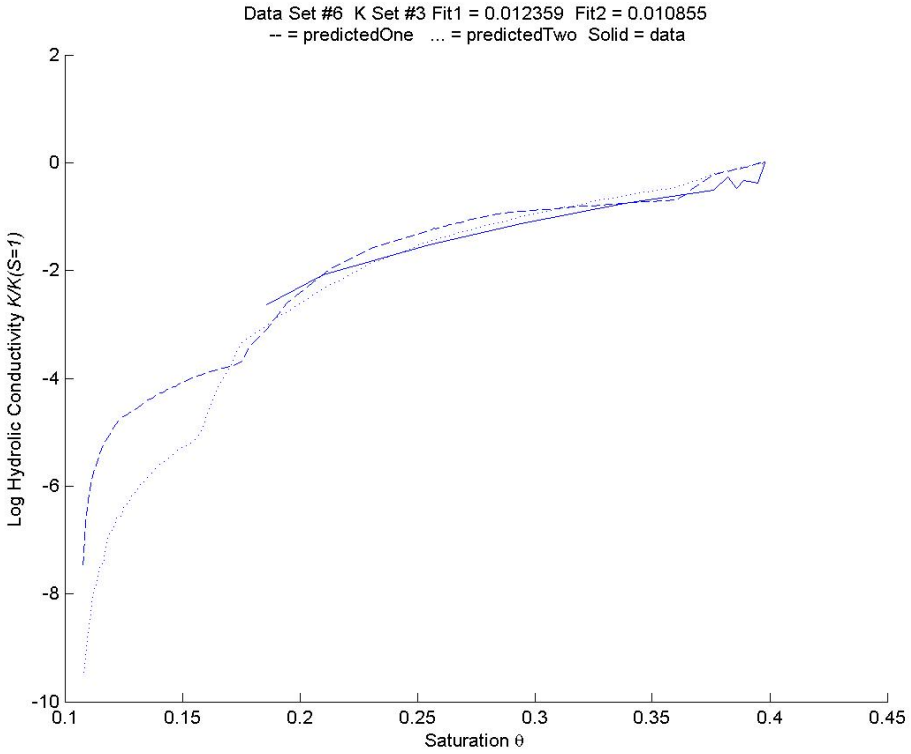

Fig R26

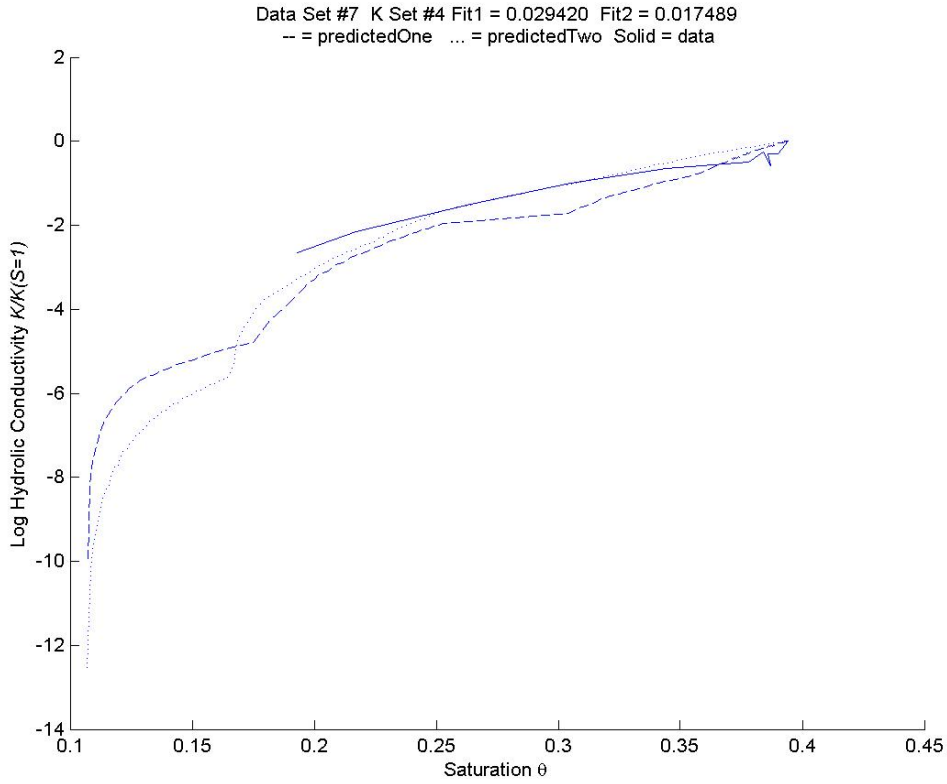

Fig R27

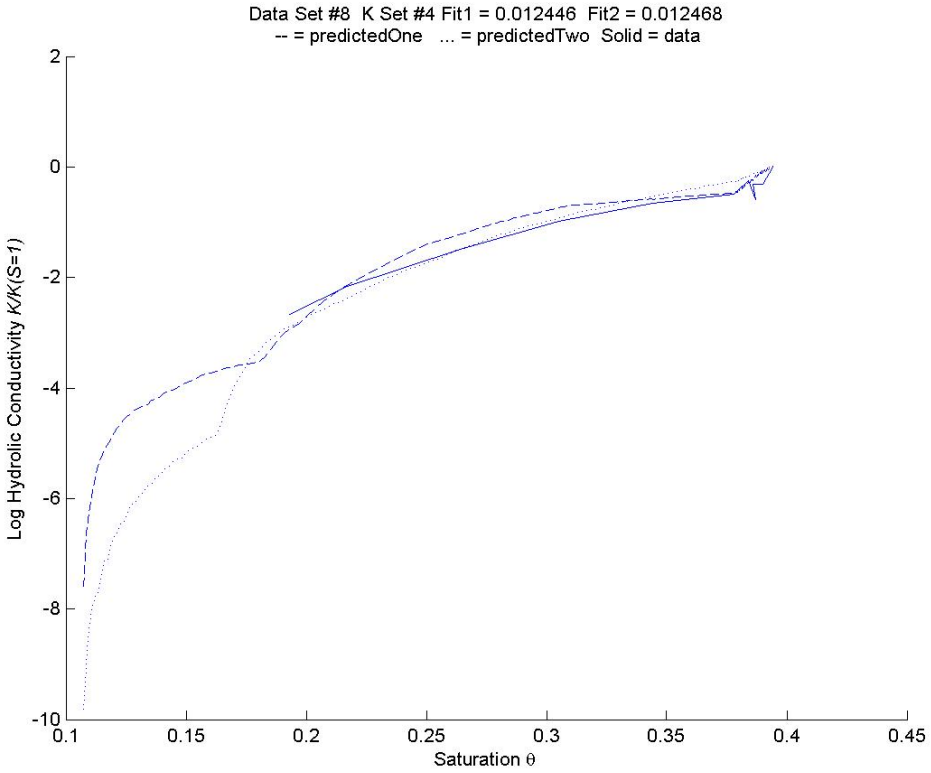

Fig R28

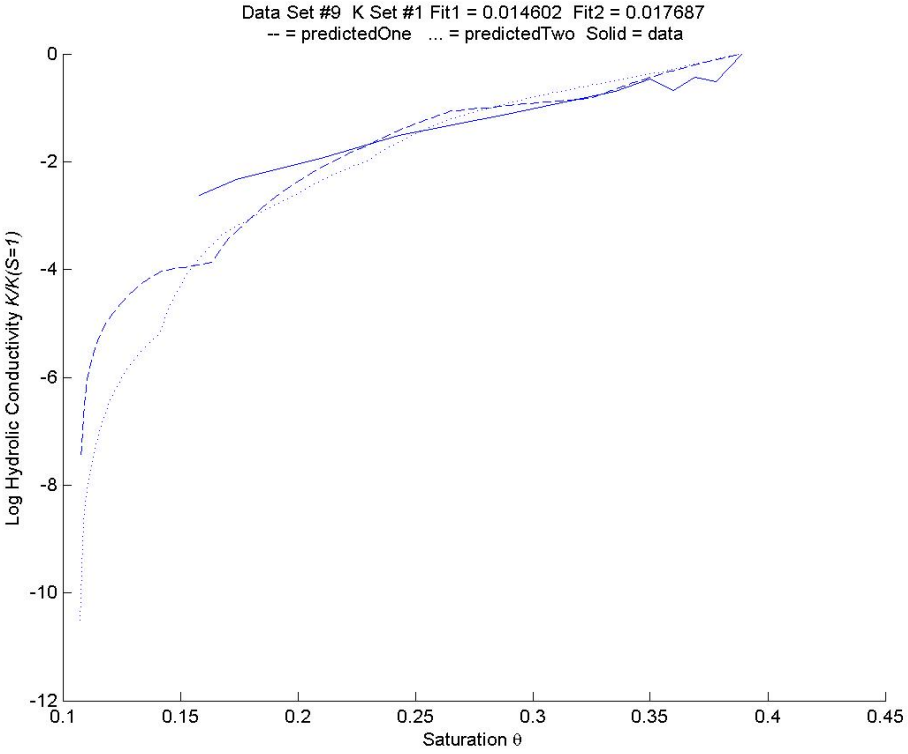

Fig R29

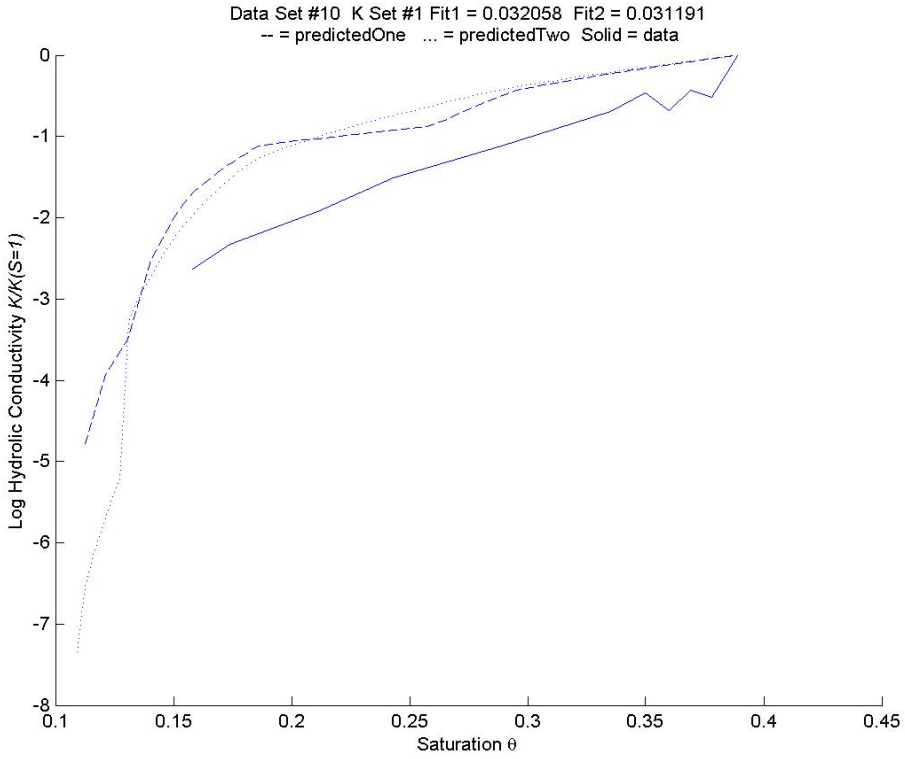

Fig R30

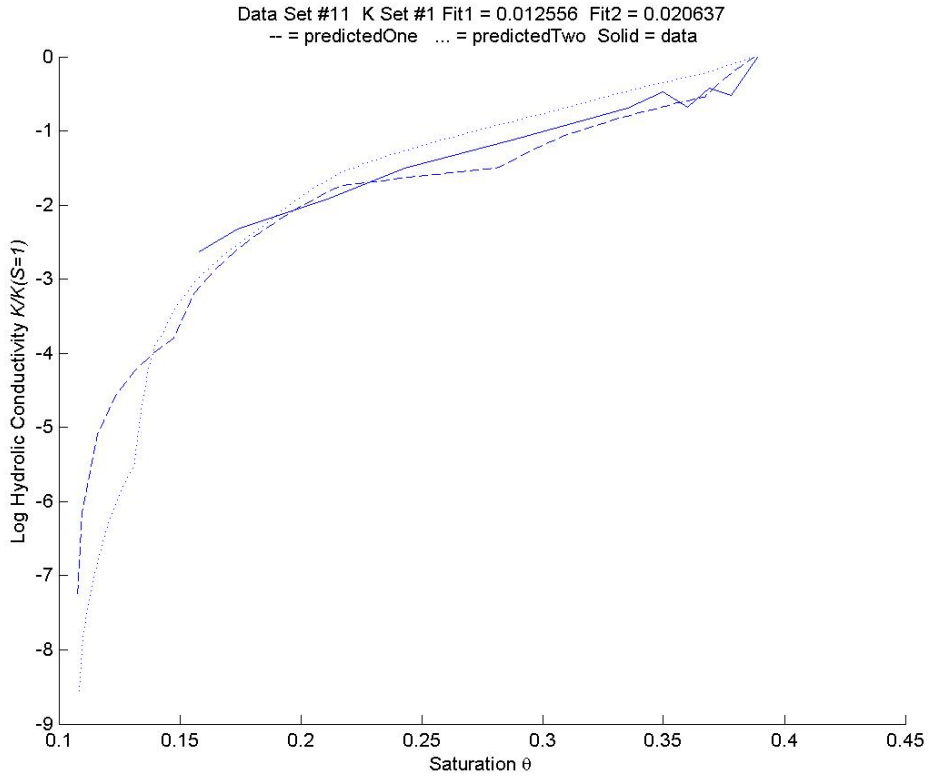

Fig R31

Table 3 summarizes the results of the least squares calculation for all eleven soil samples, each compared to all five hydraulic conductivity measurements. Each soil, compared to each set of hydraulic conductivity measurements, has two values given by the least squares routine. These two values are calculated by the two ways of binning the data , as discussed in the Data section, which were implemented in this work. Dev1 assumes R_1 is the smallest particle size in the distribution, while Dev2 assumes the smallest particle size goes to zero.

Table 3

Data Set	K1		K2		K3		K4		K5	
	RMS Dev1	RMS Dev2	RMS Dev1	RMS Dev2	RMS Dev1	RMS Dev2	RMS Dev1	RMS Dev2	RMS Dev1	RMS Dev2
1	0.02362999	0.02845532	0.02475232	0.02967975	0.0205625	0.0254018	0.01772153	0.02202945	0.02328599	0.03181162
2	0.02218951	0.0217453	0.02420236	0.02427464	0.02116217	0.02327693	0.01734629	0.02165189	0.02622499	0.03599453
3	0.01449357	0.0145871	0.01466393	0.01515839	0.01688228	0.01606031	0.01782764	0.01549659	0.02737314	0.02698829
4	0.01726347	0.01141314	0.01909778	0.0128043	0.01562383	0.01104688	0.01442129	0.01073809	0.02213568	0.01666392
5	0.0481956	0.02853869	0.0510752	0.03065171	0.04605761	0.02660678	0.04186733	0.02280603	0.04012991	0.03018847
6	0.0120112	0.01213524	0.0121607	0.01373479	0.01235865	0.01085545	0.01432543	0.0110301	0.0223926	0.01993601
7	0.03688204	0.02298146	0.03983303	0.02506063	0.03529658	0.02065077	0.02941986	0.01748862	0.03045697	0.02840385
8	0.01040143	0.01552383	0.01312013	0.01668839	0.01178568	0.01335099	0.01244636	0.01246804	0.02375487	0.02303269
9	0.01460246	0.01768723	0.01560318	0.01951361	0.01662423	0.01856121	0.01644312	0.01661633	0.02781578	0.02953399
10	0.03205813	0.03119111	0.03510598	0.03322872	0.03497946	0.03357514	0.03722788	0.03550678	0.04704388	0.04443257
11	0.01255582	0.02063713	0.01617557	0.0208352	0.01366871	0.02236629	0.01421052	0.02461822	0.01763034	0.03604271

The lack of data for K for the Rockhold (2005) data set restricts our comparison with experimental data to a single site (McGee Ranch), which would tend to emphasize the role of coincidence in any statistical analysis. In other words, to get a more realistic idea of the scope of validity of the treatment one needs a much wider database. On the other hand, the predictions of the water retention curves, for which we have a much broader range of data, do not constitute the sought-for validation of the percolation theoretical treatment of K, as the non-equilibrium effects treated by Hunt and Skinner in the fractal case have not yet been incorporated into the general model.

The predicted values of the hydraulic conductivity also tend to deviate at the very lowest moisture contents, and we believe that this occurs for a similar reason. In order to

measure such low values of the hydraulic conductivity in field studies, the study must be conducted over months or years, but this is prohibitively expensive.

Given the known experimental limitations at low water contents, as well as the general variability in data, it appears that the theoretical curves for K may be predictive. It is worth noting that phenomenologies currently in use (Mualem, 1976; van Genuchten, 1980) typically fail to predict $K(\theta)$ by several orders of magnitude in the vicinity of θ_d Their strength is that they can describe a very wide range of data phenomenologically through curve-fitting, but they are not expected to be predictive (Hunt, 2004).

Remaining questions regarding whether the pore-space can generally be modeled from knowledge of the particle sizes have not been addressed. This is the major uncertainty in modeling water retention curves using the method in this thesis. It appears that this assumption was reasonably verified here (with the possible exception of curves…R3, R5, R13, R14…), but it is already common knowledge that such an assumption breaks down for very coarse soils. It is also not clear in advance where it will work and where it will fail. Note also that there was no obvious correlation between particle size distributions or experimental treatment for curves R3, R5, R13, and R14.

Conclusions

A study was conducted to test the predictions of critical path analysis for the hydraulic conductivity, *K*, in an arbitrary porous medium. *K* was obtained as a function of saturation and also pressure. Particle size data were used to infer the pore space characteristics, a procedure which, though commonly used in this field, is not often tested quantitatively. Data for *K* were taken from the US DOE Hanford site and compared with our predictions. The results of this study found:

1. Using particle data to predict pore geometry often, but by no means always, generates water-retention curves that qualitatively reproduce the data.
2. Using concepts of percolation theory to predict the ratio of the unsaturated to the saturated hydraulic conductivity appears to be very successful for the data set analyzed. Predictions over as many as four orders of magnitude of *K* were typically within a half an order of magnitude of observed values.
3. The method developed for calculating *K* from particle-size data can be applied to any porous medium when both the particle size distribution and the critical moisture content for percolation are known. If the pore-size distribution is not accurately generated from the particle size distribution, the method will not give accurate results.
4. Although final confirmation would require many further tests, this method shows promise of being the first accurate means to predict the hydraulic conductivity as a function of saturation in disordered porous media.

References

Arya, L. M. and J. F. Paris, 1981, A physicoempirical model to predict the soil moisture characteristic from particle-size distribution and bulk density data, Soil Sci. Soc. Am. J. 45: 1023-1080.

Ambegaokar, V. N., B. I. Halperin, and J. S. Langer, 1971, Hopping conductivity in disordered systems, Phys. Rev. B, 4: 2612-2621.

Baveye, P., J.-Y. Parlange, and B. A. Stewart (ed.), 1998. Fractals in Soil Science, CRC Press, Boca Raton, FL.

Berkowitz, B. and I. Balberg, 1993, Percolation theory and its application to groundwater hydrology, Water Resour. Res. 29: 775-794.

Broadbent, S. R., and J. M. Hammersley, 1957, Percolation processes, 1. Crystals and mazes, Proc. Cambridge Philos. Soc., **53**: 629-641

Buckingham, E., 1907, Studies on the movement of soil moisture, U.S. Department of Agriculture, Bureau of Soils, Bulletin 38.

Burdine, N. T., 1953, Relative permeability calculations from pore-size distribution data, Petrol. Trans. Am Inst. Min. Eng. 198: 71-77.

Carman, P.C., 1956, Flow of Gases Through Porous Media, Butterworths, London.

Childs, E. C., and N. Collis-George, 1950, The permeability of porous materials, Proc. Royal Soc. London, Ser. A 201: 392-405.

Fisher, M. E., 1971, in Critical Phenomena, Enrico Fermi Summer School, ed. M. S. Green, Academic Press, New York, p. 1.

Gee, G.W., and J.W. Bauder. 1986. Particle-size analysis. p. 383–411. *In* A. Klute. (ed.) *Methods of soil analysis. Part 1*. 2nd ed. Agron. Monogr. 9. ASA and SSSA, Madison, WI.

Gvirtzman, H. and P. V. Roberts, 1991, Pore scale spatial analysis of two immiscible fluids in porous media. *Water Resour. Res.*, **27**: 1167.

Halliday, Resnick, Walker, 2004, Fundamentals of Physics 7th Extended Edition, Wiley, Hoboken.

Hunt, A. G., 2001, Applications of Percolation Theory to Porous Media with Distributed Local Conductances, *Advances in Water Resources* **24(3,4)**, 279-307.

Hunt, A. G., 2004, Comparing van Genuchten and percolation theoretical formulations of the hydraulic properties of unsaturated media, Vadose Zone Journal, 3: 1483-1488.

Hunt, A. G., 2005, Percolation theory for flow in porous media, Springer, Berlin.

Hunt, A. G., and G. W. Gee, 2002a, Water retention of fractal soil models using continuum percolation theory: Tests of Hanford site soils, Vadose Zone Journal, 1: 252-260.

Hunt, A. G., and G. W. Gee, 2002b, Applications of critical path analysis to fractal porous media: Comparison with examples from the Hanford site, Advances in Water Resources, 25: 129-146.

Hunt, A. G., and T. E. Skinner, 2005, Hydraulic conductivity limited equilibrium: Effect on water-retention characteristics, Vadose Zone Journal, 2, 759-765.

Hunt, A. G., L. A. Blank, and T. E. Skinner, 2006, Distributions of the Hydraulic Conductivity for Single-Scale Anisotropy, *Philosophical Magazine*, **86**: 2407-2428.

Kozeny, J., 1927, Ueber Kapillare Leitung des Wassers im Boden, Zitzungsber. Akad. Wiss. Wien, 136: 271-306.

Marshall, T. J., J. W. Holmes, C. W. Rose, 1996, *Soil Physics*, 3rd Edition, 469 pages ISBN:0521451515 | ISBN13:9780521451512.

Miller, E. E., and R. W. Miller, 11956, Physical theory for capillary flow phenomena, J. Appl. Phys. 27: 324-332.

Millington, R. J., and J. P. Quirk, 1959, Permeability of porous media, Nature (London) 183: 387-388.

Moldrup, P., T. Oleson, T. Komatsu, P. Schjoning, and D. E. Rolston, 2001, Tortuosity, diffusivity, and permeability in the soil liquid and gaseous phases, Soil Sci. Soc. Am. J. 65: 613-623.

Mualem, Y., 1976, A new model for predicting the hydraulic conductivity of unsaturated porous media, Water Resour. Res., 12: 513-522.

Nigmatullin, R. R., L. A. Dissado, and n. N. Soutougin, 1992, A fractal pore model for Archie's law in sedimentary rocks, *J. Phys. D. Appl. Phys*. **25**: 32-37.

Opportunities in the Hydrologic Sciences, Committee on Opportunities in the Hydrologic Sciences, Water Science and Technology Board, Commission on Geosciences, Environment, and Resources, National Research Council: National Academy Press, Washington, D.C., 1991.

Pollak, M., 1972, A percolation treatment of dc hopping conduction, J. Non-Cryst. Solids, 11: 1-24.

Rieu, M., and G. Sposito, 1991, Fractal fragmentation, soil porosity, and soil water properties I: Theory. Soil Sci. Soc. Am. J., 55: 1231.

Rockhold, M. L., M. J. Fayer, and G. W. Gee, 1988, Characterization of unsaturated hydraulic conductivity af the Hanford site, PNL 6488 Pacific Northwest National Laboratory, Richland, WA 99352.

Sahimi, M. and Y. C. Yortsos, 1990, Applications of fractal geometry to porous media: A review, Paper presented at the 1990 Annual Fall Meeting of the Society of Petroleum Engineers, New Orleans, LA.

Sahimi, M., 1993, Flow phenomena in rocks - From continuum models to fractals, percolation, cellular-automata, and simulated annealing. *Rev Mod Phys* **65** (4): 1393-1534

Scher, H. and R. Zallen, 1970, Critical density in percolation processes, J. Chem. Phys. 53: 3759.

Seager, C. H. and G. E. Pike, 1974, Percolation and conductivity: A computer study II. Phys. Rev. B 10: 1435-46.

Snyder, V., 1996, Statistical hydraulic conductivity models and scaling of capillary phenomena in porous media, Soil Sci. Solc Am. J. 60: 771-774.

Stauffer, Dietrich and Aharony, Amnon, 1994, Introduction to Percolation Theory. Taylor & Francis.

Stauffer, D., 1979, Scaling theory of percolation clusters, Physics Reports, 54: 1-74.

Topp, G. C., A. Klute, and D. B. Peters, 1967, Comparison of water content-pressure head data obtained by equilibrium, steady-state and unsteady state methods. *Soil Sci. Soc. Am. Proc*. 31: 312-314.

Tyler, S. W. and S. W. Wheatcraft, 1990, Fractal processes in soil water retention, Water Resour. Res. 26: 1045-1054.

Turcotte, D. L., 1986, Fractals and fragmentation, J. Geophys. Res. 91: 1921-1926.

Van Genuchten, M. Th., 1980, A closed form equation for predicting the hydraulic conductivity of unsaturated soils, Soil Sci. Soc. Am. J., 44: 892-898.

Ward AL, ME Conrad, WD Daily, JB Fink, VL Freedman, GW Gee, GM Hoversten, JM Keller, EL Majer, CJ Murray, MD White, SB Yabusaki, and ZF Zhang. 2006. Vadose Zone Transport Field Study: Summary Report . PNNL-15443, Pacific Northwest National Laboratory, Richland, WA.

Wikipedia. "Percolation Theory" http://en.wikipedia.org/wiki/Percolation_theory

Wildenschild, D., J. W. Hopmans, 1999, Flow rate dependence of hydraulic properties of unsaturated porous media, In: Characterization and Measurement of the Hydraulic Properties of Unsaturated Porous Media, ed. M. Th. van Genuchten, F. J. Leij, and L. Wu, U.S. Salinity Laboratory, Agricultural Research Service, U.S. Department of Agriculture, Riverside, CA. p. 893-904.